INCORPORATION OF
A NEW PBL PARAMETERIZATION INTO
A GENERAL CIRCULATION MODEL

by

Celal S. Konor
Department of Atmospheric Science, Colorado State University, Colorado,
Akio Arakawa
Department of Atmospheric and Oceanic Sciences, UCLA, California

April 2008

Corresponding author address: Dr. Celal S. Konor, Department of Atmospheric Science, Colorado State University, Fort Collins, CO 80523-1371. *E-mail:* csk@atmos.colostate.edu

ABSTRACT

This technical report presents a detailed description of a new PBL parameterization incorporated into the UCLA-GCM.

The PBL parameterization presented here is an extension of the parameterization already used in the UCLA-GCM based on a single mixed layer with variable depth (Randall, 1976 and Suarez et al., 1983). The new version uses multiple layers while approximately maintaining the advantages of the original parameterization. In this parameterization, the bulk formulation is used for the effects of convectively active large eddies and a newly introduced K-closure formulation is used for the effects of diffusive small eddies. The bulk formulation, which is originally introduced by Randall, Branson, Zhang, Moeng and Krasner (unpublished, partially based on Krasner, 1993), is based on a predicted bulk turbulence kinetic energy and explicitly determined PBL-top entrainment. The entrainment formulation used in this parameterization is discussed by Randall and Schubert (2004) and Stevens (2002).

Table of Contents

1. Introduction
2. Basic equations
3. Vertically discrete equations for the PBL
4. Bulk PBL parameterization
5. K-closure formulation
6. Summary

1. Introduction

It has been widely recognized that the planetary boundary layer (PBL) plays a crucial role in the climate system. The representation of PBL processes, however, remains one of the major unresolved issues in climate modeling due to the complexity of the physical processes involved. The situation is especially serious for the PBL with a stratocumulus cloud layer inside.

The scale of turbulence in the PBL can be classified into two categories: the quasi-local small eddies and the non-local large eddies. This has led to two separate approaches in the formulation of PBL processes in atmospheric models: one emphasizes the small eddies by parameterizing their effects through a K-closure formulation (Louis, 1979) and the other emphasizes the large eddies by parameterizing their effects through a bulk approach, which implicitly includes the diffusive effects by assuming a well-mixed PBL (Lilly, 1968). In later years, the K-closure formulation has been extended to include non-local effects by skewing the K-profile and including a countergradient flux term (Troen and Mahrt, 1986; Holtzlag and Moeng, 1991; Holtslag and Boville, 1993).

The behavior and structure of the clear convective PBL is relatively well understood and, therefore, its realistic simulation is the starting point of any comprehensive PBL parameterization. It is widely accepted that the two approaches mentioned above perform reasonably well in simulating major aspects of clear PBL. If the PBL top is higher than the condensation level, a cloudy sublayer forms within the PBL near the top. In this sublayer, turbulence is primarily driven by the convection due to the radiative cooling near the cloud top. Therefore, the cloud-topped PBL can be maintained even without positive buoyancy due to a

surface heat flux. The mixed-layer approach comprises a straightforward formulation of turbulence fluxes in such a PBL (Lilly, 1968) while the K-closure approach does not.

A PBL parameterization based on the mixed-layer approach complemented by Deardorff's (1972) bulk parameterization for the variable-depth PBL is incorporated into the UCLA GCM (Randall 1976, Suarez et al. 1983). In this model, the layer next to the lower boundary is designated as the PBL, which acts as a well-mixed layer (see Fig. 1a). The parameterized mass entrainment (detrainment) into (out of) the PBL at the PBL top contributes to the rate of change of the PBL depth. The PBL temperature, moisture and wind fields are predicted using the parameterized surface fluxes and the fluxes associated with the entrainment (or detrainment) through the PBL top.

The use of a variable-depth well-mixed PBL greatly simplifies parameterization of PBL cloud processes. In particular, formulation of physical processes concentrated near the cloud top is much more tractable with this approach. The successful simulation of time-averaged stratocumulus cloud incidence with a recent version of the UCLA GCM (Li et al. 1999) is largely due to this advantage. The approach has disadvantages, however, some of which are listed below. First, it does not allow the vertical variation of the horizontal velocity within the PBL. Vertical resolution required for representing low-level baroclinicity, therefore, may be lost, especially when the PBL is deep. Moreover, even conservative thermodynamic variables, such as the moist static energy and the total water mixing ratio, which are assumed to be well-mixed in the bulk approach, are not always well-mixed in reality, especially for the stable PBL. Secondly, an inevitable large jump in the vertical resolution between the PBL and the layer above in high vertical resolution models can cause large truncation errors.

The majority of climate models do not explicitly treat the PBL clouds. Among the ones with explicit treatment, for example, Gordon and Stern (1982) and Sud and Walker (1992) use an empirical formulation based on relative humidity; Hansen et al. (1983) uses a prognostic cloud water formulation; Suarez et al. (1983), Randall et al. (1989) and the model we present here use the mixed-layer approach for the treatment of PBL clouds. A comprehensive review about the performance of the PBL cloud treatments can be found in Wyngaard and Moeng (1990). More recently, Lock et al. (2000) developed a formulation in which the treatment is based on an extended empirical relative humidity formulation. Lock's scheme is now used in the UKMO and GFDL models.

In recent years, there are efforts to incorporate the variable-depth PBL approach in the models based on the local and non-local K-formulations to improve the simulation of PBL cloud incident (Beljaars and Viterbo, 1998; Lock et al., 2000; Grenier and Bretherton, 2001). In these applications, the PBL is not an explicit model layer such as the one discussed in previous two paragraphs, but the PBL depth is diagnosed or predicted, locating the PBL-top anywhere between the levels of the model that are more or less fixed in space. Then, the PBL-top jump is generally obtained through an extrapolation technique from above and below. In this approach, therefore, the difficulty in maintaining a physically consistent PBL-top jump remains as a major problem.

An interesting approach gaining momentum is the mass-flux concept based on a convective circulation model (see Arakawa 1969, Arakawa 2000). The concept has been applied to the PBL parameterization problem for more than three decades by several authors. Most recent examples are Lappen and Randall (2001a,b,c), Bretherton et al. (2004), McCaa and Bretherton (2004), Soares et al. (2004) and Siebesma et al. (2007). The mass-flux concept

appears to be useful in parameterizing the horizontal structure of the PBL, especially in determining the horizontal cloud distribution in transition from stratus to stratocumulus regimes. We recognize this approach as complimentary to the parameterization we discuss in this here.

In this technical note, we propose a hybrid approach that introduces multiple model layers within the PBL to resolve its internal structure, while retaining the advantages of the bulk parameterization (see Fig. 1b). In this approach, the bulk formulation is used for the effects of convectively active large eddies, and a K-closure formulation is used for the effects of diffusive small eddies as in Randall (1976). Simulated profiles in the PBL are allowed to deviate from well-mixed profiles. The deviations are, however, assumed to be small for thermodynamic conservative variables in formulating bulk properties of the PBL.

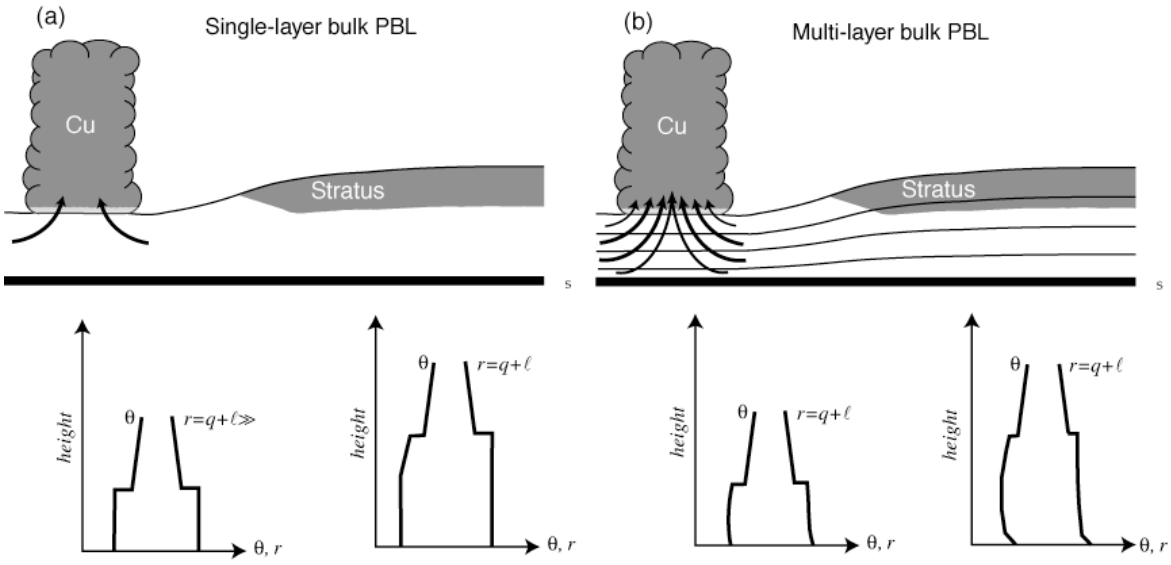

Fig. 1. Schematic representation of parameterized PBL a) based on a single layer as in current UCLA GCM and b) based on the multi-layers. Lower panel illustrates typical vertical profiles of the potential temperature θ and the total water mixing ratio r.

We implemented this approach in vertically discrete models, using a vertical coordinate system in which the PBL-top is a coordinate surface shared by both the free atmosphere and

the PBL. In this way, as we mentioned earlier, the formulation of the processes that are highly concentrated near the PBL top becomes more explicit. When the PBL does not have a well-defined top, such as the left-over "daytime" PBL in evening, the definition of this coordinate system becomes ambiguous. In such a situation, the coordinate can be viewed as an arbitrarily chosen coordinate.

A major advantage of such a hybrid parameterization is in the simulation of the PBL processes during the surface frontogenesis. The multi-layer formulation allows vertical wind shears to be developed and maintained within the PBL due to the vertically varying pressure gradient force, while the potential temperature is nearly well mixed in the vertical. In this way, we may expect more realistic simulations of extratropical cyclones and better prediction of low-level cloud distributions in the middle latitudes with this parameterization.

The PBL-top entrainment (or detrainment), PBL cloud processes and the surface fluxes are formulated following a new approach based on the predicted bulk turbulence kinetic energy (TKE), originally introduced by Randall, Branson, Zhang, Moeng and Krasner (1998, personal communications; hereafter, RBZMK). The most important aspects of this approach can be found in Krasner (1993), Zhang et al. (1996), Randall et al., (1998) and Randall and Schubert (2004). The bulk properties of the PBL to be used in our formulations are obtained by mass-weighted vertical averaging of the prognostic variables over the entire PBL. In the case of potential temperature, averaging is only over the sub-cloud layers.

We incorporated the multi-layer PBL parameterization into the UCLA GCM. The results obtained by selected climate simulations will be presented in a forthcoming paper.

In the next section, we discuss the basic governing equations for the free-atmosphere/PBL system. We discuss the vertical discretization of the equations for the PBL in

section 3. The bulk PBL parameterization, which represents the effects of large convective eddies, are discussed in section 4. In section 5, we discuss the K-closure formulation representing the effects of the small diffusive eddies. Finally, a summary is presented in section 6.

2. Continuous governing equations of the AGCM

a. Vertical coordinate

The vertical coordinate system used in the model is presented in Suarez *et al*. (1983). The vertical domain is divided into three regions (Fig. 2), the boundaries of which are coordinate surfaces. The highest region extends from the model's top ($p_T = 1\text{hPa}$) to the mean

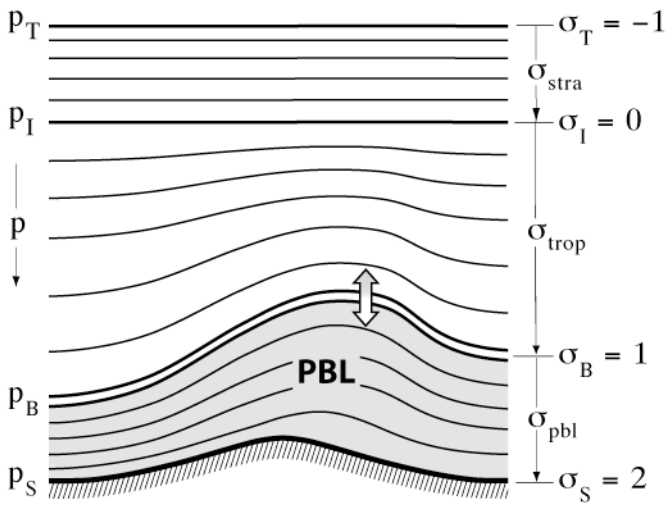

Fig. 2. Vertical structure and sigma coordinate of the model.

tropopause level ($p_I = 100\text{ hPa}$). The middle region extends from the mean tropopause level down to the PBL top, p_B, which varies in space and time. The lowest region represents the PBL. Within these regions, the definition of vertical sigma coordinate is given by,

$$\sigma_{STRA} \equiv (p - p_I)/(p_I - p_T) \qquad \text{for } p_T \le p \le p_I, \tag{2.1a}$$

$$\sigma_{TROP} \equiv (p - p_I)/(p_B - p_I) \qquad \text{for } p_I \le p \le p_B \tag{2.1b}$$

and

$$\sigma_{PBL} \equiv 1 + (p - p_B)/(p_S - p_B) \quad \text{for } p_B \le p \le p_S \tag{2.1c}$$

where p is pressure and p_S the surface pressure. Accordingly, $\sigma = 2$ at the Earth's surface, $\sigma = 1$ at the PBL top, $\sigma = 0$ at the mean tropopause level, and $\sigma = -1$ at the model's top. The coordinate surface at the PBL top ($\sigma = 1$) represents an infinitesimally thin transition layer (*a.k.a.* inversion layer) that separates the PBL air below from the free atmosphere air above.

In general the mass variable is defined by

$$m \equiv \frac{\partial p}{\partial \sigma}. \tag{2.2}$$

From (2.1a) to (2.1c), we obtain corresponding mass variables for three vertical regions as

$$m_{STRA} \equiv (p_I - p_T)/(\sigma_I - \sigma_T) \text{ for } \sigma_T \le \sigma \le \sigma_I, \tag{2.3a}$$

$$m_{TROP} \equiv (p_B - p_I)/(\sigma_B - \sigma_I) \text{ for } \sigma_I \le \sigma \le \sigma_B \tag{2.3b}$$

and

$$m_{PBL} \equiv (p_S - p_B)/(\sigma_S - \sigma_T) \text{ for } \sigma_B \le \sigma \le \sigma_S, \tag{2.3c}$$

respectively. Note that m_{STRA} is a constant and, according to the selection of σ given above, $(\sigma_I - \sigma_T) = (\sigma_B - \sigma_I) = (\sigma_S - \sigma_B) = 1$.

b. Mass continuity equation

In general, the continuity equation for a σ vertical coordinate is given by

$$\left(\frac{\partial}{\partial t}\right)_\sigma m + \nabla_\sigma \cdot (m\mathbf{v}) + \frac{\partial}{\partial \sigma}(m\dot{\sigma}) = 0, \tag{2.4}$$

where ∇_σ is the horizontal del operator taken along constant σ surfaces, $\mathbf{v}$ the horizontal velocity and $\dot{\sigma}$ the "vertical σ velocity" defined by

$$\dot{\sigma} \equiv \frac{D\sigma}{Dt} . \tag{2.5}$$

In (2.4), $m\dot{\sigma}$ is the vertical mass flux trough coordinate surface. The material time derivative in (2.5) is defined by

$$\frac{D}{Dt} \equiv \left(\frac{\partial}{\partial t} \right)_{\sigma} + \mathbf{v} \cdot \nabla_{\sigma} + \dot{\sigma} \frac{\partial}{\partial \sigma} . \tag{2.6}$$

For mass conservation, we assume that there is no vertical mass fluxed at the model top and the surface,

$$\left(m\dot{\sigma} \right)_T = \left(m\dot{\sigma} \right)_S = 0 . \tag{2.7}$$

If we apply (4) to three vertical regions, we obtain

$$\nabla_{\sigma} \cdot \left(m_{STRA} \mathbf{v} \right) + \frac{\partial}{\partial \sigma} \left(m\dot{\sigma} \right) = 0 \qquad \text{for } \sigma_T \le \sigma \le \sigma_I , \tag{2.8a}$$

$$\frac{\partial m_{TROP}}{\partial t} + \nabla_{\sigma} \cdot \left(m_{TROP} \mathbf{v} \right) + \frac{\partial}{\partial \sigma} \left(m\dot{\sigma} \right) = 0 \qquad \text{for } \sigma_I \le \sigma \le \sigma_B , \tag{2.8b}$$

and

$$\frac{\partial m_{PBL}}{\partial t} + \nabla_{\sigma} \cdot \left(m_{PBL} \mathbf{v} \right) + \frac{\partial}{\partial \sigma} \left(m\dot{\sigma} \right) = 0 \qquad \text{for } \sigma_B \le \sigma \le \sigma_S , \tag{2.8c}$$

respectively. Note that the continuity equation for the uppermost region (2.8a) becomes a diagnostic equation that is used to determine the vertical mass flux. The pressure tendency equations can be obtained by vertical integration of (2.8b) and (2.8c) and using (2.3b) and (2.3c) as

$$\left.\begin{aligned} &\left(\frac{\partial}{\partial t}\right)_\sigma p + \int_{\sigma_I}^{\sigma} \nabla_\sigma \cdot \left(m_{TROP}\mathbf{v}\right) d\sigma + \left(m\dot{\sigma}\right) - \left(m\dot{\sigma}\right)_I = 0 \quad for\ \sigma_I \le \sigma < \sigma_B \\ &\frac{\partial p_B}{\partial t} + \int_{\sigma_I}^{\sigma_B} \nabla_\sigma \cdot \left(m_{TROP}\mathbf{v}\right) d\sigma + \left(m\dot{\sigma}\right)_B - \left(m\dot{\sigma}\right)_I = 0 \quad for\ \sigma = \sigma_B \end{aligned}\right\} \tag{2.9a}$$

and

$$\left.\begin{aligned} &\left(\frac{\partial}{\partial t}\right)_\sigma p - \frac{\partial p_B}{\partial t} + \int_{\sigma_B}^{\sigma} \nabla_\sigma \cdot \left(m_{TROP}\mathbf{v}\right) d\sigma + \left(m\dot{\sigma}\right) - \left(m\dot{\sigma}\right)_B = 0 \quad for\ \sigma_B < \sigma < \sigma_S \\ &\frac{\partial p_S}{\partial t} - \frac{\partial p_B}{\partial t} + \int_{\sigma_B}^{\sigma_S} \nabla_\sigma \cdot \left(m_{PBL}\mathbf{v}\right) d\sigma - \left(m\dot{\sigma}\right)_B = 0 \quad for\ \sigma = \sigma_S \end{aligned}\right\}. \tag{2.9b}$$

In deriving (2.9a) from (4), we assumed $\left(\partial p_T/\partial t\right) = 0$ and $\left(m\dot{\sigma}\right)_T = 0$. In (2.9b), we used $\left(m\dot{\sigma}\right)_S = 0$. The determination of the vertical mass fluxes will be discussed later.

c. Thermodynamic equation

The thermodynamic equation can be generally written as

$$\left(\frac{\partial}{\partial t}\right)_\sigma \left(m\theta\right) + \nabla_\sigma \cdot \left(\theta m\mathbf{v}\right) + \frac{\partial}{\partial \sigma}\left(\theta m\dot{\sigma}\right) = \frac{mQ}{\Pi}, \tag{2.10}$$

where θ is the potential temperature, Q the diabatic heating per unit mass, $\Pi \equiv c_p\left(p/p_0\right)^\kappa$ the Exner function, c_p the specific heat of dry air under constant pressure, p_0=1000hPa the standard pressure, $\kappa \equiv R/c_p$, R the gas constant for dry air. For PBL, the thermodynamic equation is given by

$$\left(\frac{\partial}{\partial t}\right)_\sigma \left(m_{PBL}\theta\right) + \nabla_\sigma \cdot \left(\theta m_{PBL}\mathbf{v}\right) + \frac{\partial}{\partial \sigma}\left(\theta m\dot{\sigma}\right) = \frac{m_{PBL}Q}{\Pi} + g\frac{\partial F_\theta}{\partial \sigma} + G_\theta, \tag{2.11}$$

where g is the gravitational acceleration, F_θ the turbulent flux of potential temperature and G_θ the additional effects. Positive values of F_θ correspond to upward fluxes. The determination of the turbulent fluxes and the additional effects will be discussed later.

d. Moisture equation

The model predicts the water vapor mixing ratio q for the free atmosphere (top two regions) from

$$\left(\frac{\partial}{\partial t}\right)_\sigma (mq) + \nabla_\sigma \cdot (qm\mathbf{v}) + \frac{\partial}{\partial \sigma}(qm\dot{\sigma}) = -mC\,, \tag{2.12}$$

where C is the condensation rate for unit mass. For the PBL, the model predicts the total water mixing ratio r from

$$\left(\frac{\partial}{\partial t}\right)_\sigma (m_{PBL} r) + \nabla_\sigma \cdot (rm_{PBL}\mathbf{v}) + \frac{\partial}{\partial \sigma}(rm\dot{\sigma}) = -m_{PBL}\mathcal{R} + g\frac{\partial F_r}{\partial \sigma} + G_r\,, \tag{2.13}$$

where $\mathcal{R}$ is the rain drop generation rate, F_r the turbulent flux of total water and G_r represents additional effects. Positive values of F_r correspond to upward fluxes. Note that $r = q + \ell$, where ℓ is the liquid water mixing ratio. The liquid water mixing ratio can be obtained from $\ell = r - q^*$ and $q = q^*$ if $r > q^*$, where q^* is the saturation mixing ratio.

e. Momentum equation

The momentum equation for the free atmosphere is given by

$$\left(\frac{\partial}{\partial t}\right)_\sigma \mathbf{v} + \mathbf{v}\cdot\nabla_\sigma\mathbf{v} + \left(\frac{\partial \mathbf{v}}{\partial \sigma}\right)\dot{\sigma} = -\left(\nabla_p \Phi\right) - f\mathbf{k}\times\mathbf{v}\,, \tag{2.14}$$

where Φ is the geopotential height, f the Coriolis parameter and $\mathbf{k}$ the unit vector in the positive z direction. The moment equation for the PBL can be written as

$$\left(\frac{\partial}{\partial t}\right)_\sigma \mathbf{v} + \mathbf{v}\cdot\nabla_\sigma\mathbf{v} + \left(\frac{\partial \mathbf{v}}{\partial \sigma}\right)\dot{\sigma} = -\left(\nabla_p \Phi\right) - f\mathbf{k}\times\mathbf{v} + \frac{g}{m_{PBL}}\frac{\partial \mathbf{F_v}}{\partial \sigma} + \frac{\mathbf{G_v}}{m_{PBL}}, \qquad (2.15)$$

where $\mathbf{F_v}$ is the turbulent momentum flux and $\mathbf{G_v}$ the additional effects. The pressure gradient force term in (2.4) and (2.15) in a σ coordinate can be written as

$$-\nabla_p \Phi = -\nabla_\sigma \Phi + \sigma \frac{\partial \Pi}{\partial p}\frac{\partial \Phi}{\partial \Pi}\nabla m\,. \qquad (2.16)$$

The geopotential height is determined using the hydrostatic equation given by

$$\frac{\partial \Phi}{\partial \Pi} = -\theta\,. \qquad (2.17)$$

f. Vertical mass flux equation

The equation that determines the vertical mass fluxes within the uppermost region can be obtained by vertical integral of (2.8a) as

$$\left(m\dot{\sigma}\right) = -\int_{\sigma_T}^{\sigma} \nabla_\sigma \cdot \left(m_{STRA}\mathbf{v}\right) d\sigma \qquad \text{for} \quad \sigma_T \le \sigma \le \sigma_I\,. \quad (2.18)$$

Through the time derivative of (2.1b) and using (2.9a), the equation that determines the vertical mass flux in the middle region can be obtained as

$$\left(m\dot{\sigma}\right) = \sigma\left(m\dot{\sigma}\right)_B + \left(1-\sigma\right)\left(m\dot{\sigma}\right)_I + \sigma\int_{\sigma_I}^{\sigma_B} \nabla_\sigma \cdot \left(m_{TROP}\mathbf{v}\right) d\sigma - \int_{\sigma_I}^{\sigma} \nabla_\sigma \cdot \left(m_{TROP}\mathbf{v}\right) d\sigma$$

$$\text{for} \quad \sigma_I \le \sigma \le \sigma_B\,. \quad (2.19)$$

In (2.19), the PBL-top mass vertical flux is obtained from

$$\left(m\dot{\sigma}\right)_B = g\left(E - D - M_B\right), \tag{2.20}$$

where E and D are the PBL-top entrainment and detrainment rates, respectively, and M_B is the cumulus mass flux through the PBL top. For an entraining PBL, $E>0$ and $D=0$ while, for a detraining PBL, $D>0$ and $E=0$. In (2.19), $\left(m\dot{\sigma}\right)_I$ is obtained from (2.18). Finally, following the procedure used to obtain (2.19), the vertical mass flux within the PBL can be obtained as

$$\left(m\dot{\sigma}\right) = \left(2-\sigma\right)\left(m\dot{\sigma}\right)_B + \left(\sigma-1\right)\int_{\sigma_B}^{\sigma_S} \nabla_\sigma \cdot \left(m_{PBL}\mathbf{v}\right) d\sigma - \int_{\sigma_B}^{\sigma} \nabla_\sigma \cdot \left(m_{PBL}\mathbf{v}\right) d\sigma$$

$$\text{for} \quad \sigma_B \le \sigma \le \sigma_S . \tag{2.21}$$

Note that $\sigma_I = 0$ and $\sigma_B = 1$ in (2.19), and $\sigma_I = 0$ in (2.21).

g. Determination of turbulent flux of potential temperature in the PBL

The potential temperature θ is not a conserved quantity for a saturated atmosphere due to the condensation heating. On the other hand, the moist static energy ($h \equiv \Pi\theta + \Phi + L_c q$ and $h^* \equiv \Pi\theta + \Phi + L_c q^*$ for saturated air) and the total water mixing ratio r, are conserved. In this model, we first determine the turbulent fluxes of the conserved quantities h and r and then determine the turbulent flux of θ from

$$\left.\begin{aligned} F_\theta &\equiv \frac{1}{\Pi}\left(F_h - L_c F_r\right) \quad \textit{for an unsaturated layer} \\ F_\theta &\equiv \frac{1}{\Pi\left(1+\gamma^*\right)} F_h \quad \textit{for a saturated layer} \end{aligned}\right\}, \tag{2.22}$$

where F_h and F_r are the turbulent fluxes of h and r, respectively, L_c is the latent heat of condensation $\gamma^* \equiv \frac{L}{c_p}\left(\partial q^* / \partial T\right)_p$, where T is the temperature.

3. Discrete equations of the PBL

In this document, we focus on the discretization of equations for the PBL. The reader is referred to Arakawa and Suarez (1983) for the discretization of equations in the free atmosphere.

a. Vertical grid

A portion of the vertical grid for the lower free atmosphere and the PBL is shown in Fig. 3. The vertical domain of the model is divided into *M* number of layers. *L* layers from the top are assigned to the free atmosphere and *M–L* layers from the surface are assigned to the PBL. At the PBL-top, an infinitesimally thin transition layer (*a.k.a.* inversion layer) separates the PBL from the free atmosphere. The variables are staggered following the Lorenz grid.

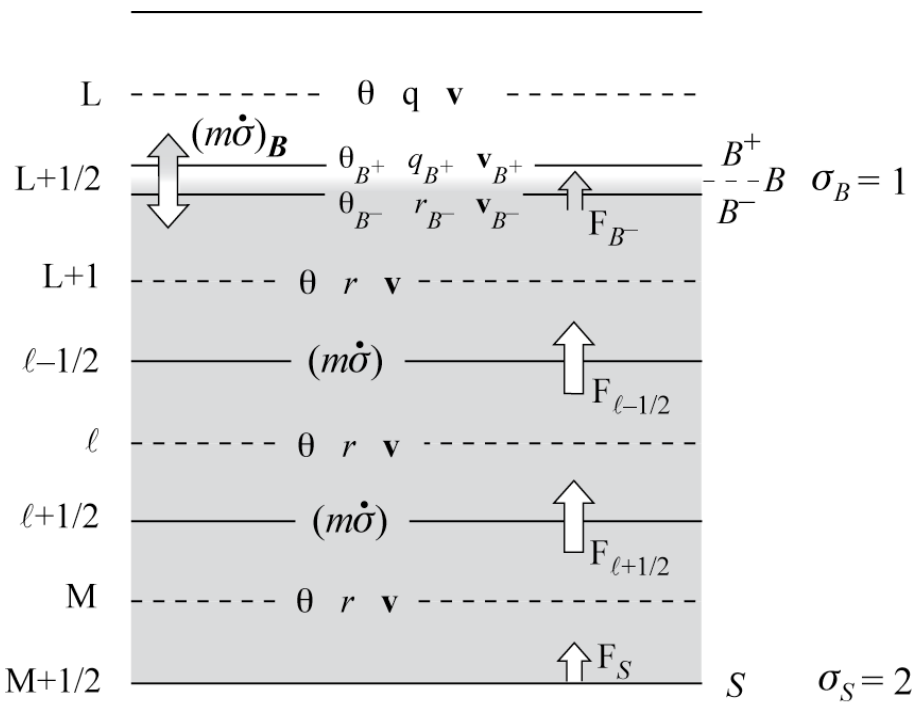

Fig. 3. Vertical grid in the PBL and lower free atmosphere.

The prognostic variables are placed at the model layers and, turbulent fluxes are placed at the interfaces of those layers. The quantities at the upper boundary of the transition layer (B^+) are obtained by an extrapolation from the lowest two layers of the free atmosphere. The values of conserved quantities, such as total water mixing ratio and moist static energy, at the lower boundary of the transition layer (B^-) are assumed be equal to those at layer L+1. The potential temperature at B^- is obtained by an extrapolation from below. While this way of determining θ_{B^-} is not fully justifiable for a cloud topped PBL, it requires less computations.

b. Mass continuity equation

The discrete mass continuity equation for the PBL can be obtained by the sigma-weighted vertical sum of (2.8c) as

$$\frac{\partial m_{PBL}}{\partial t} + \frac{1}{(\delta\sigma)_{PBL}}\left[\sum_{\ell=L+1}^{M} \nabla\cdot(m\mathbf{v})_\ell (\delta\sigma)_\ell - (m\dot{\sigma})_B\right] = 0\,, \tag{3.1}$$

where

$$\left.\begin{aligned} m_{PBL} &\equiv (\delta p)_{PBL}/(\delta\sigma)_{PBL} \\ (\delta p)_{PBL} &\equiv p_{M+1/2} - p_{L+1/2} \\ (\delta\sigma)_{PBL} &\equiv \sigma_{M+1/2} - \sigma_{L+1/2} \\ (\delta\sigma)_\ell &\equiv \sigma_{\ell+1/2} - \sigma_{\ell-1/2} \quad \text{for} \quad \ell = L+1,...,M \end{aligned}\right\}. \tag{3.2}$$

To obtain (3.1), $(m\dot{\sigma})_{M+1/2} = 0$ is assumed, where $M+1/2$ and S are interchangeable. In (3.1), $(m\dot{\sigma})_B$ is the vertical mass flux at the PBL top, where B and $L+1/2$ are interchangeable. For convenience, we omit the subscript PBL in m_{PBL} hereafter. The

vertically discrete versions of pressure tendency and surface pressure tendency equations given by (2.9b) are

$$\frac{\partial p_{\ell+1/2}}{\partial t} = \frac{\partial p_B}{\partial t} - \sum_{k=L+1}^{\ell} \nabla \cdot (m_k \mathbf{v}_k)(\delta\sigma)_k - (m\dot{\sigma})_{\ell+1/2} + (m\dot{\sigma})_B \quad \text{for} \quad \ell = L+1,..,M-1 \quad (3.3a)$$

and

$$\frac{\partial p_S}{\partial t} = \frac{\partial p_B}{\partial t} - \sum_{k=1}^{L} \nabla \cdot (m_k \mathbf{v}_k)(\delta\sigma)_k + (m\dot{\sigma})_B , \quad (3.3b)$$

respectively.

c. Thermodynamic equation

The vertically discrete version of the thermodynamic equation for the PBL (2.11) applied to the model layers is given by

$$\frac{\partial (m\theta)_{L+1}}{\partial t} + \nabla \cdot (m\mathbf{v}\theta)_{L+1} + \left[\frac{\partial (m\theta\dot{\sigma})}{\partial \sigma} \right]_{L+1} = \left(\frac{mQ}{\Pi} \right)_{L+1} + \frac{g}{(\delta\sigma)_{L+1}} (F_\theta)_{L+3/2} + (G_\theta)_{L+1} \quad (3.4a)$$

and

$$\frac{\partial (m\theta)_\ell}{\partial t} + \nabla \cdot (m\mathbf{v}\theta)_\ell + \left[\frac{\partial (m\theta\dot{\sigma})}{\partial \sigma} \right]_\ell = \left(\frac{mQ}{\Pi} \right)_\ell + \frac{g}{(\delta\sigma)_\ell} \left[(F_\theta)_{\ell+1/2} - (F_\theta)_{\ell-1/2} \right] + (G_\theta)_\ell$$

$$\text{for} \quad \ell = L+2,...,M , \quad (3.4b)$$

In these equations, upward flux (F_θ) has positive values. In (3.4a), F_{B^-}, where B^- and L+1/2 are interchangeable, is implicitly considered with the vertical potential temperature flux through the PBL top. The derivation of (3.4a) and (3.4b) is discussed in Appendix A. The convergence of vertical potential temperature fluxes for the uppermost PBL layer is defined by

$$\left[\frac{\partial}{\partial\sigma}(m\theta\dot{\sigma})\right]_{L+1} \equiv \frac{1}{(\delta\sigma)_{L+1}}\left[\theta_{L+3/2}(m\dot{\sigma})_{L+3/2} - \hat{\theta}_{L+1/2}(m\dot{\sigma})_{L+1/2}\right], \tag{3.5a}$$

where

$$\left.\begin{aligned}\hat{\theta}_{L+1/2} &\equiv \theta_{B^+} \quad for \quad (m\dot{\sigma})_B > 0\\ \hat{\theta}_{L+1/2} &\equiv \theta_{B^-} \quad for \quad (m\dot{\sigma})_B < 0\end{aligned}\right\}. \tag{3.5b}$$

In (3.5b), θ_{B^+} and θ_{B^-} are obtained by extrapolations from above and below, respectively. The convergence of vertical potential temperature fluxes for other layers are defined by

$$\left[\frac{\partial}{\partial\sigma}(m\theta\dot{\sigma})\right]_{\ell} \equiv \frac{1}{(\delta\sigma)_{\ell}}\left[\theta_{\ell+1/2}(m\dot{\sigma})_{\ell+1/2} - \theta_{\ell-1/2}(m\dot{\sigma})_{\ell-1/2}\right] \text{for } \ell = L+2,...,M \tag{3.5c}$$

and

$$\left[\frac{\partial}{\partial\sigma}(m\theta\dot{\sigma})\right]_{M} \equiv -\frac{1}{(\delta\sigma)_{M}}\theta_{M-1/2}(m\dot{\sigma})_{M-1/2}. \tag{3.5d}$$

In (3.5a), (3.5c) and (3.5d), the potential temperature at the interfaces is defined by

$$\theta_{\ell+1/2} \equiv \frac{(\Pi_{\ell+1} - \Pi_{\ell+1/2})\theta_{\ell+1} + (\Pi_{\ell+1/2} - \Pi_{\ell})\theta_{\ell}}{(\Pi_{\ell+1} - \Pi_{\ell})} \qquad \text{for } \ell = L+1,...,M-1. \tag{3.6}$$

In (3.4a) and (3.4b), the turbulent fluxes (F_θ) are calculated from

$$\left.\begin{aligned}(F_\theta)_{\ell+1/2} &= \frac{1}{\Pi_{\ell+1/2}}\left[(F_h)_{\ell+1/2} - L(F_r)_{\ell+1/2}\right] \quad for\ a\ dry\ interface\\ (F_\theta)_{\ell+1/2} &= (F_h)_{\ell+1/2}\Big/\left[\Pi_{\ell+1/2}\left(1+\gamma^*_{\ell+1/2}\right)\right] \quad for\ a\ saturated\ interface\end{aligned}\right\}, \tag{3.7}$$

where $\gamma^*_{\ell+1/2} \equiv \frac{L}{c_p}\left[\left(\partial q^*/\partial T\right)_p\right]_{\ell+1/2}$, and F_h and F_r are convective eddy fluxes of moist static energy and total mixing ratio of water given by

$$\left.\begin{array}{ll} h_{\ell+1/2} = \left(\Pi\theta + \Phi + Lq\right)_{\ell+1/2} \\ r_{\ell+1/2} \equiv q_{\ell+1/2} \end{array}\right\} \quad \textit{for a dry interface}$$
$$\left.\begin{array}{ll} h_{\ell+1/2} = \left(\Pi\theta + \Phi + Lq^*\right)_{\ell+1/2} \\ r_{\ell+1/2} = q^*_{\ell+1/2} + \ell_{\ell+1/2} \end{array}\right\} \quad \textit{for a saturated interface} \qquad \Big\}, \tag{3.8}$$

respectively. In (3.8), $\theta_{\ell+1/2}$ is defined by (3.6), and the definitions of $\Phi_{\ell+1/2}$ and $r_{\ell+1/2}$ will be given later in this section. The turbulent fluxes $\left(F_h\right)_{\ell+1/2}$ and $\left(F_r\right)_{\ell+1/2}$ in (3.7) are reserved for the convective large eddies that are determined from the bulk parameterization. The turbulent flux due to small (diffusive) eddies and additional effects such as the roots of cumulus clouds are included in $\left(G_\theta\right)$. The formulation of $\left(G_\theta\right)$ will be discussed later in this text.

d. Moisture equation

From the moisture equation (2.13), the vertically discrete equation to predict the water mixing ratio *r* is given by

$$\frac{\partial(mr)_{L+1}}{\partial t} + \nabla\cdot\left(mr\mathbf{v}\right)_{L+1} + \left[\frac{\partial}{\partial\sigma}\left(mr\dot{\sigma}\right)\right]_{L+1} = -m\mathcal{R}_{L+1} + \frac{g}{\left(\delta\sigma\right)_{L+1}}\left(F_r\right)_{L+3/2} + \left(G_r\right)_{L+1} \tag{3.9a}$$

and

$$\frac{\partial(mr)_\ell}{\partial t} + \nabla\cdot\left(mr\mathbf{v}\right)_\ell + \left[\frac{\partial}{\partial\sigma}\left(mr\dot{\sigma}\right)\right]_\ell = -m\mathcal{R}_\ell + \frac{g}{\left(\delta\sigma\right)_\ell}\left[\left(F_r\right)_{\ell+1/2} - \left(F_r\right)_{\ell-1/2}\right] + \left(G_r\right)_\ell$$

$$\text{for } \ell = L+1,\ldots,M \tag{3.9b}$$

The convergence of vertical moisture fluxes for the uppermost layer in the PBL is defined by

$$\left[\frac{\partial}{\partial\zeta}(mr\dot{\sigma})\right]_{L+1} \equiv \frac{1}{(\delta\zeta)_{L+1}}\left[r_{L+3/2}(m\dot{\sigma})_{L+3/2} - \hat{r}_{L+1/2}(m\dot{\sigma})_{L+1/2}\right], \tag{3.10a}$$

where

$$\left.\begin{aligned}\hat{r}_{L+1/2} &\equiv q_{B^+} \quad for \quad (m\dot{\sigma})_B > 0\\ \hat{r}_{L+1/2} &\equiv r_{B^-} \quad for \quad (m\dot{\sigma})_B < 0\end{aligned}\right\}. \tag{3.10b}$$

In (3.10b), q_{B^+} is obtained by an extrapolation from above and $r_{B^-} \equiv r_{L+1}$. The convergence of vertical moisture fluxes for the other layers are given by

$$\left[\frac{\partial}{\partial\zeta}(mr\dot{\sigma})\right]_{\ell} \equiv \frac{1}{(\delta\zeta)_{\ell}}\left[r_{\ell+1/2}(m\dot{\sigma})_{\ell+1/2} - r_{\ell-1/2}(m\dot{\sigma})_{\ell-1/2}\right] \text{for } \ell = L+2,..,M-1 \tag{3.10c}$$

and

$$\left[\frac{\partial}{\partial\zeta}(mr\dot{\sigma})\right]_{M} \equiv -\frac{1}{(\delta\zeta)_{M}} r_{M-1/2}(m\dot{\sigma})_{M-1/2}. \tag{3.10d}$$

In (3.10a), (3.10c) and (3.10d), the total water mixing ratio at the interfaces are obtained from

$$r_{\ell+1/2} \equiv \frac{r_{\ell+1} + r_{\ell}}{2} \text{ for } \ell = L+1,...,M-1. \tag{3.11}$$

In (3.9a) and (3.9b), F_r is the turbulent fluxes due to large convective eddies. The turbulent flux due to small (diffusive) eddies and additional effects such as the roots of cumulus clouds are included in G_r. The formulation of G_r will be discussed later in this text.

e. Momentum equation

From (2.15), the vertically discrete momentum equation applied to the PBL layers can be written as

$$\frac{\partial \mathbf{v}_{L+1}}{\partial t} + \mathbf{v}_{L+1}\cdot\nabla\mathbf{v}_{L+1} + \left(\dot{\zeta}\frac{\partial \mathbf{v}}{\partial \sigma}\right)_{L+1} = -\left(\nabla_p \Phi\right)_{L+1} - f\,\mathbf{k}\times\mathbf{v}_{L+1} + \frac{g}{m_{PBL}\left(\delta\sigma\right)_{L+1}}\left(\mathbf{F}_{\mathbf{v}}\right)_{L+3/2} + \frac{\left(\mathbf{G}_{\mathbf{v}}\right)_{L+1}}{m_{PBL}} \tag{3.12a}$$

and

$$\frac{\partial \mathbf{v}_{\ell}}{\partial t} + \mathbf{v}_{\ell}\cdot\nabla\mathbf{v}_{\ell} + \left(\dot{\sigma}\frac{\partial \mathbf{v}}{\partial \sigma}\right)_{\ell} = -\left(\nabla_p \Phi\right)_{\ell} - f\,\mathbf{k}\times\mathbf{v}_{\ell} + \frac{g}{m_{PBL}\left(\delta\sigma\right)_{\ell}}\left\{\left(\mathbf{F}_{\mathbf{v}}\right)_{\ell+1/2} - \left(\mathbf{F}_{\mathbf{v}}\right)_{\ell-1/2}\right\} + \frac{\left(\mathbf{G}_{\mathbf{v}}\right)_{\ell}}{m_{PBL}}$$

$$\text{for} \quad \ell = L+2,...,M\,. \tag{3.12b}$$

In (3.12a) and (3.12b), the vertical momentum advection for the uppermost layer is defined by

$$\left(\dot{\sigma}\frac{\partial \mathbf{v}}{\partial \sigma}\right)_{L+1} \equiv \frac{1}{m\left(\delta\sigma\right)_{L+1}}\left[\frac{1}{2}\left(\mathbf{v}_{L+2} - \mathbf{v}_{L+1}\right)\left(m\dot{\sigma}\right)_{L+3/2} + \left(\mathbf{v}_{L+1} - \hat{\mathbf{v}}_{L+1/2}\right)\left(m\dot{\sigma}\right)_{B}\right], \tag{3.13a}$$

where

$$\left.\begin{aligned} \hat{\mathbf{v}}_{L+1/2} &\equiv \mathbf{v}_{B^+} \quad for \quad \left(m\dot{\sigma}\right)_B > 0 \\ \hat{\mathbf{v}}_{L+1/2} &\equiv \mathbf{v}_{B^-} \quad for \quad \left(m\dot{\sigma}\right)_B < 0 \end{aligned}\right\}. \tag{3.13b}$$

In (3.13b), $\mathbf{v}_{B^+}$ and $\mathbf{v}_{B^-}$ are obtained by extrapolations from above and below, respectively. The vertical momentum advection for the other layers is defined by

$$\left(\dot{\sigma}\frac{\partial \mathbf{v}}{\partial \sigma}\right)_{\ell} \equiv \frac{1}{2m\left(\delta\sigma\right)_{\ell}}\left[\left(\mathbf{v}_{\ell+1} - \mathbf{v}_{\ell}\right)\left(m\dot{\sigma}\right)_{\ell+1/2} + \left(\mathbf{v}_{\ell} - \mathbf{v}_{\ell-1}\right)\left(m\dot{\sigma}\right)_{\ell-1/2}\right] \quad \text{for} \quad \ell = L+1,..,M-1$$

(3.13c)

and

$$\left(\dot{\sigma}\frac{\partial \mathbf{v}}{\partial \sigma}\right)_M \equiv \frac{1}{2m(\delta\sigma)_M}(\mathbf{v}_M - \mathbf{v}_{M-1})(m\dot{\sigma})_{M-1/2}. \qquad (3.13d)$$

where the subscript PBL is omitted in m_{PBL}. In (3.13a), (3.13c) and (3.13d), $(\mathbf{F}_\mathbf{v})_{L+3/2}$ and $(\mathbf{F}_\mathbf{v})_{\ell+1/2}$ are the turbulent momentum fluxes due to large convective eddies. $(\mathbf{G}_\mathbf{v})_{L+3/2}$ and $(\mathbf{G}_\mathbf{v})_{\ell+1/2}$ represent the additional effects such as the turbulent fluxes due to the small (diffusive) eddies and roots of cumulus clouds. Formulations of these terms will be discussed later in this text.

The vertically discrete version of the pressure gradient force (2.16) is given by

$$-\left(\nabla_p\Phi\right)_\ell = -\nabla\Phi_m - \frac{1}{m\left(\sigma_{\ell+1/2}-\sigma_{\ell-1/2}\right)}\left(\Phi_{\ell-1/2}-\Phi_{\ell+1/2}\right)\left(\nabla p_B\right)$$

$$-\frac{(\nabla m)}{m\left(\sigma_{\ell+1/2}-\sigma_{\ell-1/2}\right)}\left[\sigma_{\ell+1/2}\left(\Phi_\ell-\Phi_{\ell+1/2}\right)+\sigma_{\ell-1/2}\left(\Phi_{\ell-1/2}-\Phi_\ell\right)-\sigma_B\left(\Phi_{\ell-1/2}-\Phi_{\ell+1/2}\right)\right]. \qquad (3.14)$$

Note that (3.14) for a single becomes identical to the pressure gradient force term introduced by Suarez *et al*. (1983). Derivation of (3.14) is given in Appendix B.

The vertically discrete version of the hydrostatic equation (2.17) within the PBL is given by

$$\Phi_\ell = \Phi_{\ell+1} + \left(\Pi_{\ell+1}-\Pi_{\ell+1/2}\right)\theta_{\ell+1} + \left(\Pi_{\ell+1/2}-\Pi_\ell\right)\theta_\ell \quad \text{for } \ell = M-1,..L+1 \qquad (3.15a)$$

and, at the lower layer,

$$\Phi_M = \Phi_S + \left(\Pi_S - \Pi_M\right)\theta_M. \qquad (3.15b)$$

In these equations, the Exner function for the model layers are defined by

$$\Pi_\ell \equiv \frac{p_{\ell+1/2}\Pi_{\ell+1/2} - p_{\ell-1/2}\Pi_{\ell-1/2}}{\left(R/c_p + 1\right)\left(p_{\ell+1/2} - p_{\ell-1/2}\right)}. \tag{3.16}$$

The pressure for the layers can be obtained from $p_\ell \equiv p_o \Pi_\ell^{1/\kappa} / c_p$.

f. Vertical mass flux equation

The discrete version of the vertical mass flux equation for the PBL (2.21) can be written as

$$\left(m\dot{\sigma}\right)_{\ell+1/2} = \left(\sigma - 1\right)\sum_{k=1}^{L} \nabla\cdot\left(m_k \mathbf{v}_k\right)\left(\delta\sigma\right)_k - \sum_{k=L+1}^{\ell} \nabla\cdot\left(m_k \mathbf{v}_k\right)\left(\delta\sigma\right)_k + \left(2-\sigma\right)\left(m\dot{\sigma}\right)_B$$

$$\text{for } \ell = L+1,\ldots,M-1. \tag{3.17}$$

At the PBL-top, the vertical mass flux is determined by

$$\left(m\dot{\sigma}\right)_B = g\left(E - D - M_B\right), \tag{5.26}$$

where E and D are the PBL-top entrainment and detrainment rates, respectively, and M_B is the upward cumulus mass flux through the PBL top. For an entraining PBL, $E > 0$ and $D = 0$ while, for a detraining PBL, $D > 0$ and $E = 0$. The entrainment E and M_B are determined by the bulk PBL and the cumulus parameterizations, respectively.

4. Discretization of PBL processes

a. Turbulence fluxes due to large convective eddies

It is assumed that the turbulence fluxes of **v**, *h* and *r* due to large convective eddies change linearly in the vertical within PBL. If ψ represents **v**, *h* or *r*, the flux for the interface ℓ+1/2 within the PBL can be written as

$$\left(F_\psi\right)_{\ell+1/2} = \left(\sigma_{\ell+1/2} - \sigma_B\right)\left(F_\psi\right)_S + \left(\sigma_S - \sigma_{\ell+1/2}\right)\left(F_\psi\right)_{B^-} \qquad \text{for } \ell = L+1, \cdots, M-1, \quad (4.1)$$

where $\left(F_\psi\right)_S$ and $\left(F_\psi\right)_{B^-}$ are the surface and PBL-top fluxes at level B^- of ψ determined by the bulk parameterization discussed later in this text. According to the coordinate used in this model, $\sigma_B = 1$ and $\sigma_S = 2$.

b. Turbulence fluxes due to small eddies

In the hybrid PBL parameterization being described here, the turbulent flux $\tilde{F}$ due to small eddies is determined through a K-closure formulation given by

$$\left(\tilde{F}_\psi\right)_{L+1/2} = 0, \qquad (4.2a)$$

$$\left(\tilde{F}_\psi\right)_{\ell+1/2} \equiv -\rho_{\ell+1/2} K_{\ell+1/2}\left[\frac{\psi_{\ell+1} - \psi_\ell}{(\delta z)_{\ell+1/2}} - \left(\gamma_T\right)_{\ell+1/2}\right] \text{ for } \ell = L+1, \cdots, M-1 \quad (4.2b)$$

$$\left(\tilde{F}_\psi\right)_{M+1/2} \equiv 0 \qquad (4.2c)$$

where ψ represents **v**, *h* or *r*, ρ is the density, *K* the diffusion coefficient, $(\delta z)_{\ell+1/2} \equiv z_\ell - z_{\ell+1}$ and γ_T the transport. Similar to (3.17), the fluxes of the potential temperature can be written as

$$\left.\begin{aligned} \left(\tilde{F}_\theta\right)_{\ell+1/2} &= \frac{1}{\Pi_{\ell+1/2}}\left[\left(\tilde{F}_h\right)_{\ell+1/2} - L_c\left(\tilde{F}_r\right)_{\ell+1/2}\right] \quad & \textit{for a dry interface} \\ \left(\tilde{F}_\theta\right)_{\ell+1/2} &= \left(\tilde{F}_h\right)_{\ell+1/2} \Big/ \left[\Pi_{\ell+1/2}\left(1+\gamma^*_{\ell+1/2}\right)\right] \quad & \textit{for a saturated interface} \end{aligned}\right\}. \qquad (4.3)$$

Note that, for a dry interface, $\left(\tilde{F}_q\right)_{\ell+1/2} = \left(\tilde{F}_r\right)_{\ell+1/2}$.

c. Effects of small eddies, cumulus mass flux and radiation

This subsection describes the discretization of additional effects (*G*) in the thermodynamic, moisture and momentum equations. If ψ represents **v**, θ or *r*, the additional effects can be included by

$$\left(G_\psi\right)_{L+1} \equiv \frac{g}{\left(\delta\sigma\right)_{L+1}}\left[-\left(\tilde{F}_\psi\right)_{L+3/2} + \lambda_{L+1}^{(c)}\left(\psi_{B^+} - \psi_{B^-}\right)M_B - \left(R_\psi\right)_{B^+}\right], \tag{4.4a}$$

$$\left(G_\psi\right)_{\ell} \equiv \frac{g}{\left(\delta\sigma\right)_{\ell}}\left[-\left(\tilde{F}_\psi\right)_{\ell+1/2} + \left(\tilde{F}_\psi\right)_{\ell-1/2} + \lambda_{\ell}^{(c)}\left(\psi_{B^+} - \psi_{B^-}\right)M_B\right] \text{ for } \ell = L+2,\cdots,M-1 \tag{4.4b}$$

and

$$\left(G_\psi\right)_{M} \equiv \frac{g}{\left(\delta\sigma\right)_{M}}\left[\left(\tilde{F}_\psi\right)_{M-1/2} + \lambda_{M}^{(c)}\left(\psi_{B^+} - \psi_{B^-}\right)M_B\right]. \tag{4.4c}$$

A detailed derivation of (4.4a) to (4.4c) is given in Appendix A. The determination of ψ_{B^+} and ψ_{B^-} is discussed above in this section for each quantities. In (4.4a), $\left(R_\psi\right)_{B^+}$ is the upward radiation flux of ψ at B^+. For $\psi \equiv \theta$, R_{B^+}, where we ignore the subscript, represents the net longwave radiation. There is no radiative transfer of the momentum and moisture, $\left(R_{\mathbf{v}}\right)_{B^+} = \left(R_r\right)_{B^+} = 0$. The effect of cumulus roots is also incorporated through $\lambda_\ell^{(c)}\left(\psi_{B^+} - \psi_{B^-}\right)M_B$, where $\lambda_\ell^{(c)}$ is the fractional contribution factor satisfying $\sum_{\mathrm{m}=L+1}^{M} \lambda_{\mathrm{m}}^{(c)} = 1$.

4. Bulk PBL parameterization

Here we describe the bulk PBL parameterization originally described by Randall, Branson, Zhang, Moeng and Krasner (RBZMK, 1998, unpublished manuscript). In this parameterization, i) the bulk turbulence kinetic energy (TKE) for the PBL is predicted, ii) the square root of the predicted TKE is used for the bulk velocity in determining the surface fluxes, and iii) an explicit formulation based on the predicted TKE is used to determine the PBL-top entrainment rate. Additionally, this parameterization has a simplified PBL-top entrainment instability formulation, which is incorporated into the expression that determines the entrainment rate.

As in Suarez et al. (1983), we consider three regimes for the PBL as schematically shown in Fig. 4. The first regime is the clear deepening PBL such as clear daytime PBL over

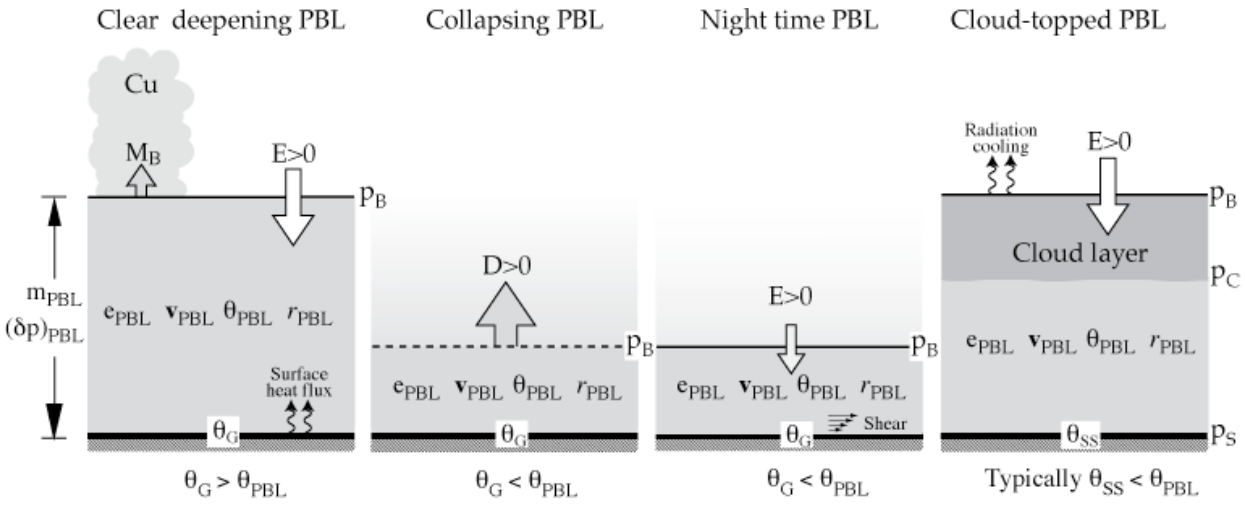

Fig. 4. Schematic representation of the different PBL regimes considered in the PBL parameterization. The subscripts G and SS denote ground and sea surface, respectively, and they can be used interchangeably.

land. In this regime, the TKE increases typically due to the buoyancy generated by the warming of Earth's surface due to solar heating, and consequently the PBL tends to deepen by entraining air from the free atmosphere. The second regime is the night-time situation over

land. After sunset, due to the sudden loss of the buoyancy generation, the TKE decreases and then the PBL collapses, leaving a large part of PBL air to the free atmosphere. Unlike the deepening PBL case, there is no well-defined PBL top during this transition, which is this difficult to simulate in a discrete model. Yet, this process is an essential part of the PBL-free atmosphere interaction. For that reason, we pay a special care on realistically simulating this process in our model. The technique we used will be discussed later in this text. After this transition, the PBL typically starts deepening again with a relatively slow rate due to the shear contribution to the TKE generation during the night-time. In the parameterization we also consider the cloud-topped PBL regime, which is often observed over the colder oceans of the cost of California and Peru and over the high-latitude snow-covered land. In this regime, the TKE is maintained by the buoyancy generated by radiative cooling near the top of the cloud layer.

a. Determination of bulk quantities for multi layer PBL

Suarez et al. (1983) predicts the PBL velocity, the potential temperature and the total water mixing-ratio for the *subcloud layer* of the PBL. Unlike their parameterization, here we predict the velocity, potential temperature, total water mixing ratio for each of the multiple layers within the PBL. Therefore, we must define the bulk properties to be used in the bulk parameterization. We define a bulk value of ψ denoted by ψ_{PBL} as

$$\psi_{PBL} \equiv \frac{1}{\int_{p_B}^{p_S} \eta dp} \int_{p_B}^{p_S} \eta\psi(p)dp, \tag{4.1}$$

where

$$\eta \equiv \begin{cases} 1 & for \quad r < q^*(T,p) \\ 0 & for \quad r \geq q^*(T,p) \end{cases}. \tag{4.2}$$

If the entire PBL is saturated, we define $\psi_{PBL} = \psi(p_S)$. In the discrete system, we first interpolate the quantities into a high vertical resolution grid and then use (4.1) and (4.2) to determine the bulk quantities θ_{PBL} and r_{PBL} for the entire PBL.

b. Bulk turbulence kinetic energy equation

The bulk turbulence kinetic energy (TKE) for the mixed-layer e_{PBL} is predicted by

$$\frac{\partial e_{PBL}}{\partial t} = -\frac{e_{PBL}}{(\delta p)_{PBL}} gE + \frac{g}{(\delta p)_{PBL}}(\mathcal{B} + S - \mathcal{D}) + \frac{e_{PBL}}{m}\nabla \cdot (m\mathbf{v}), \tag{4.3}$$

where $(\delta p)_{PBL} = p_S - p_B$, E is the entrainment rate, $\mathcal{B}$ is the buoyancy generation, S is the shear generation, $\mathcal{D}$ is the dissipation of TKE and m is the mass of the PBL defined by $m \equiv (\delta p)_{PBL}/(\sigma_S - \sigma_B)$. Reader is referred to Krasner (1993) for the detail derivation of (4.3). Some aspect of the derivation of (4.3) is discussed in Appendix C. The buoyancy generation is given by

$$\mathcal{B} \equiv \int_{p_B}^{p_S} \frac{\kappa F_{\mathbf{sv}}}{p} dp, \tag{4.4}$$

where F_{sv} is the turbulent flux of virtual dry static energy defined by $s_v = \Pi\theta_v + \Phi$, where θ_v is the virtual potential temperature, which is defined by $\theta_v \equiv T_v(p/p_o)^{\kappa}$. T_v is the virtual temperature is defined by $T_v \equiv T(1 + 0.608\,q - \ell)$, where q and ℓ are the mixing ratios of water vapor and liquid water, respectively. The shear generation is formally given by

$$S \equiv \int_{z_S}^{z_B} \mathbf{F}_\mathbf{v} \cdot \frac{\partial \mathbf{v}}{\partial z} dz , \tag{4.5}$$

where $\mathbf{F}_\mathbf{v}$ is the turbulent momentum flux. In our model, however, we only consider low-level shear to calculate S, which will be discussed later in this text. The dissipation of TKE in (4.3) is expressed by

$$\mathcal{D} \equiv C \rho_{PBL} \left(e_{PBL} \right)^{3/2} , \tag{4.6}$$

where C is a constant ($C \approx 1$ according to Moeng and Sullivan, 1994), which remains to be determined, and ρ_{PBL} is the averaged density in the PBL given by $\rho_{PBL} \equiv (\delta p)_{PBL} / (\Phi_B - \Phi_S)$.

Equation (4.3) is valid only for the "turbulent (deepening) state", for which formally $e_{PBL} > 0$ (in our model, $e_{PBL} > e_{min}$). If there is a tendency toward $e_{PBL} < e_{min}$, it is assumed that the mixed-layer is in "collapsing state", for which we let $e_{PBL} = e_{min}$ and $(\delta p)_{PBL} = (\delta p)_{min}$, where e_{min} and $(\delta p)_{min}$ are properly chosen lower limits of e_{PBL} and $(\delta p)_{PBL}$, respectively. The PBL maintains the "collapsed state" until $e_{PBL} > e_{min}$ again. We are currently using $(\delta p)_{min} = 10$ hPa and $e_{min} = 10^{-3}$ m^{2}sec^2.

c. Determination of surface fluxes

The surface fluxes of momentum, heat and moisture are defined by

$$\left.\begin{aligned} \left(\mathbf{F}_\mathbf{v}\right)_S &\equiv -\rho_S C_U C_U \, \mathrm{Max}\left\{\alpha_1 |\mathbf{v}_M|, \beta_1 e_{PBL}^{1/2}\right\} \mathbf{v}_M \\ \left(F_\theta\right)_S &\equiv \rho_S C_U C_T \, \mathrm{Max}\left\{\alpha_2 |\mathbf{v}_M|, \beta_2 e_{PBL}^{1/2}\right\} (\theta_S - \theta_M) \\ \left(F_q\right)_S &\equiv \rho_S C_U C_T \, \mathrm{Max}\left\{\alpha_2 |\mathbf{v}_M|, \beta_2 e_{PBL}^{1/2}\right\} \left[q^*(T_S, p_S) - q_M \right] k \end{aligned}\right\} , \tag{4.7}$$

where ρ_S is the density at the lowest PBL layer, C_U and C_T the surface exchange coefficients computed following Deardorff (1972), **v** the vector wind velocity, the subscript *M* denotes the lowermost PBL layer, e_{PBL} the TKE, θ_S Earth's surface potential temperature, T_S the surface temperature, p_S the surface pressure and *k* a coefficient that represents the ground wetness. The coefficient *k* takes the value of one for water surfaces, and a value close to zero for arid lands. The parameters α_1, β_1 , α_2 and β_2 are scale coefficients empirically determined to obtain realistic simulated fluxes. We are currently using $\alpha_1 = 1.0$, $\beta_1 = 5.5$, $\alpha_2 = 0.7$, $\beta_2 = 4.0$. Reader is referred to Zhang et al. (1996) for the use of the square root of TKE as the velocity scale in the surface flux formulation.

d. Determination of bulk turbulent fluxes, buoyancy and PBL-top entrainment

A) Clear deepening PBL (typically $\theta_G > \theta_{PBL}$):

Typical vertical profiles of *r, q,* θ, $s \equiv \Pi\theta + \Phi$, *h* and *h** are shown in Fig. 5 for clear deepening PBL. Note that, for this case, *r* = *q*.

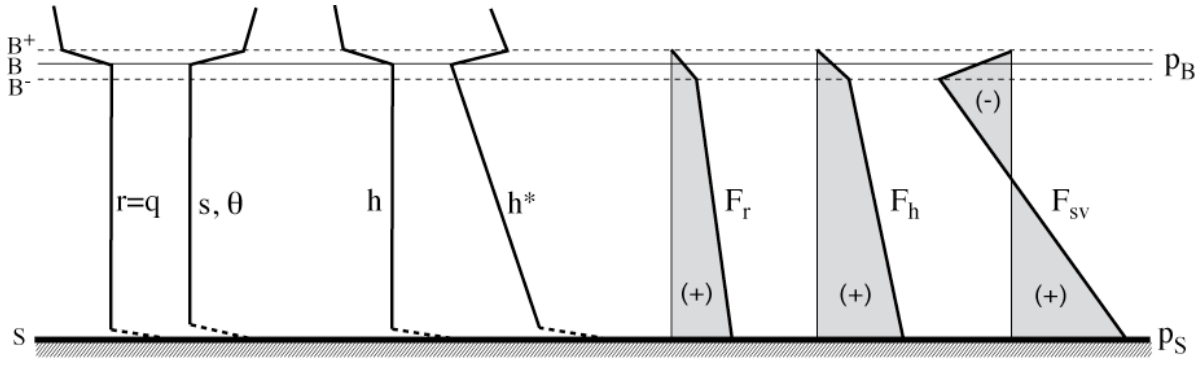

Fig. 5. Typical vertical profiles of r, q, θ, s, h, h*, F_r, F_h and F_{sv} for clear deepening PBL.

Within the PBL, the conserved quantities, namely *q,* θ*, s* and *h,* are vertically well mixed while

*h** decreases nearly linearly with height. The turbulence fluxes of the total water F_r and moist static energy $F_h \equiv \Pi F_\theta + LF_r$, where $\Pi F_\theta = F_s$, are positive and linearly decreases with height from their surface values, $(F_r)_S$ and $(F_h)_S = \Pi_S (F_\theta)_S + L(F_r)_S$, respectively. The surface fluxes $(F_\theta)_S$ and $(F_r)_S \equiv (F_q)_S$ are given by (4.7) and the PBL-top fluxes are given by

$$\left.\begin{aligned}(F_r)_{B^-} &= -E(\Delta r)_B \\ (F_h)_{B^-} &= -E(\Delta h)_B\end{aligned}\right\}, \tag{4.8}$$

where $(\Delta)_B \equiv (\ )_{B^+} - (\ )_{B^-}$. The turbulence flux of the virtual dry static energy F_{sv}, which is given by $F_h + (0.608\Pi\theta_{PBL} - L)F_r$ or $\Pi F_\theta + 0.608\Pi\theta_{PBL}F_r$, linearly decreases with height from a positive value at the surface, $(F_{sv})_S > 0$, to a negative value at the PBL-top, $(F_{sv})_{B^-} < 0$. There is a well-established empirical relationship between $(F_{sv})_S$ and $(F_{sv})_{B^-}$ for clear deepening PBL given by

$$(F_{sv})_{B^-} = -k(F_{sv})_S, \tag{4.9}$$

where $k \approx 0.2$. The buoyancy generation (4.4) for this case becomes

$$\mathcal{B} \approx \kappa\left[(F_{sv})_S + (F_{sv})_{B^-}\right](p_S - p_B)/(p_S + p_B), \tag{4.10}$$

where

$$\left.\begin{aligned}(F_{sv})_{B^-} &= (F_h)_{B^-} + (0.608\Pi_B\theta_{PBL} - L)(F_r)_{B^-} = \Pi_B(F_\theta)_{B^-} + 0.608\Pi_B\theta_{PBL}(F_r)_{B^-} \\ (F_{sv})_S &= (F_h)_S + (0.608\Pi_S\theta_{PBL} - L)(F_r)_S \quad = \Pi_S(F_\theta)_S + 0.608\Pi_S\theta_{PBL}(F_r)_S\end{aligned}\right\}. \tag{4.11}$$

In (4.11), we used $\Pi_B(F_\theta)_{B^-} = (F_\theta)_{B^-} - L(F_r)_{B^-}$ and $r \equiv q$. Following RBZMK (1998,

unpublished manuscript), the PBL-top entrainment is determined from

$$E \approx \left(\frac{2kC}{1-k}\right)\frac{\rho_{PBL}\sqrt{\tilde{e}_{PBL}}}{\dfrac{g\left(\Delta s_v\right)_B\left(\delta z\right)_{PBL}}{e_{PBL}\Pi_B\theta_{PBL}}}, \tag{4.12}$$

where $\tilde{e}_{PBL} \equiv e_{PBL} - e_{min}$. We assume that $\left(\Delta s_v\right)_B = \Pi_B\left(\Delta\theta\right)_B + 0.608\left(\Delta r\right)_B$ is positive and use the typical value of $C \approx 1$ (see Moeng and Sullivan, 1994). A detailed derivation process of (4.12) is given in Appendix D.

B) Collapsing PBL (typically $\theta_G < \theta_{PBL}$):

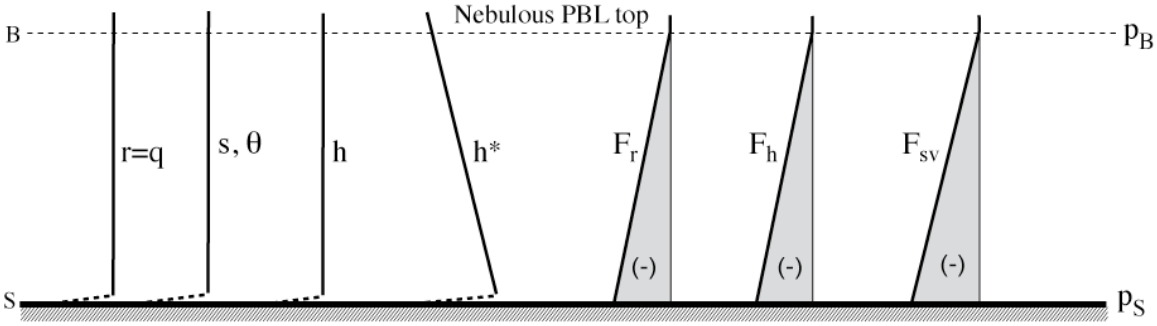

Fig. 6. Typical vertical profiles of r, q, θ, s, h , h*, F_r, F_h and F_{sv} for collapsing PBL.

For the collapsing case, the TKE is nearly zero and, therefore, the PBL is not well defined so that we choose $\left(\Delta h\right)_B = \left(\Delta r\right)_B = 0$. The turbulence fluxes are typically negative (see Fig. 6). In our model, we assume that the PBL air detrains through its prognostically determined top with a finite rate while the TKE is set to its minimum value, $e_{PBL} = e_{min}$. The detrainment rate *D* is calculated from an arbitrary relationship given by

$$D \equiv \frac{(\delta p)_{max}}{g\,\tau_{collapse}}, \tag{4.13}$$

where we use values for $(\delta p)_{max}$ and $\tau_{collapse}$ given by 250 mb and 3 hours, respectively.

C) Nighttime PBL ($\theta_G < \theta_{PBL}$):

After the collapse of the PBL, the TKE starts increasing again due to the shear contribution. We treat this regime similar to the clear deepening PBL except the TKE here is generated by the shear rather than the buoyancy.

D) Cloud-topped PBL (typically $\theta_{SS} < \theta_{PBL}$):

A cloud layer forms in the upper PBL if the condensation level denoted by C is lower than the PBL-top. The height of the condensation level can be determined by

$$p_C \equiv p_B + (p_S - p_B)\frac{r_{PBL} - q^*_{B0}}{q^*_S - q^*_{B0}}, \tag{4.14}$$

where $q^*_S = q^*(T_S, p_S)$, $q^*_{B0} = q^*(T_{B0}, p_B)$, $T_S \equiv \Pi_S \theta_{PBL}/c_p$ and $T_{B0} \equiv \Pi_B \theta_{PBL}/c_p$ (see Fig. 7).

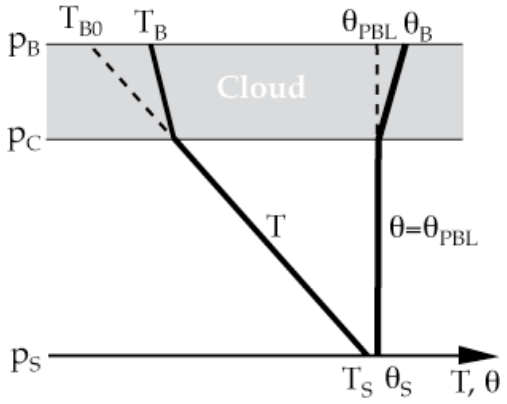

Fig. 7. Typical vertical profiles of the temperature T and the potential temperature θ in a cloud-topped PBL.

In this case, only in subcloud layer, θ and s are conserved and, therefore, there are constant. Within the cloud layer, θ and s generally increase with height (see Fig. 8) while r

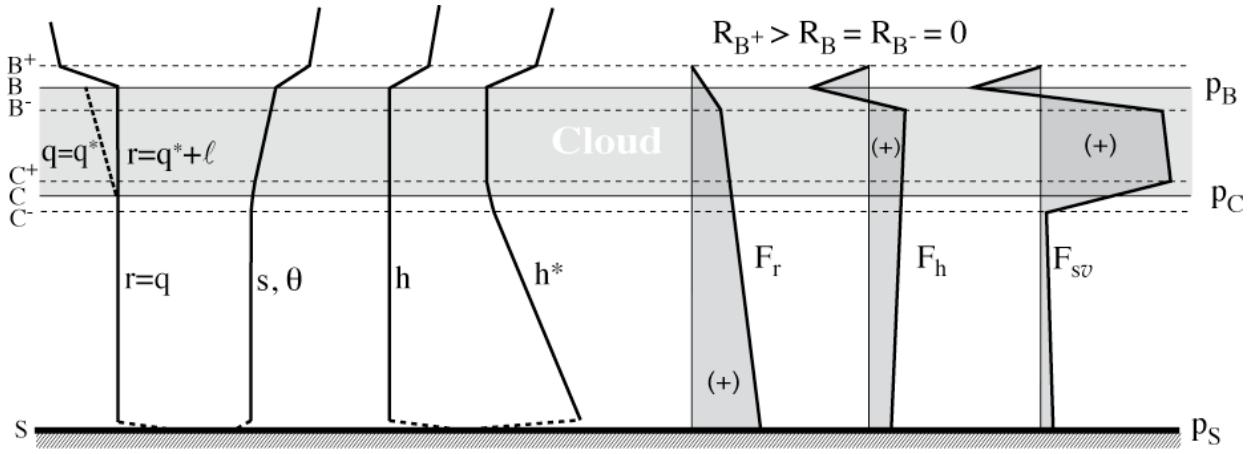

Fig. 8. Typical vertical profiles of r, q, θ, s, h , h*, F_r, F_h and F_{sv} for cloud-topped PBL.

and h remain uniform throughout the PBL. F_{sv} is usually negative in the subcloud layer if the surface is colder than the PBL. It is generally positive in the cloud layer, however, due to turbulence generated by radiative cooling near the top of the cloud. We can define the fluxes as follows:

Within the cloud layer ($p<p_C$):

$$F_{sv} \equiv F_s + \Pi\theta\left(0.608F_q - F_\ell\right), \tag{4.15}$$

Within the cloud layer, the air is saturated, in which the liquid water-mixing ratio is given by $\ell \equiv r - q^*$. We define the fluxes on the right hand side of (4.15) as

$$F_s = F_h - L_c F_{q^*} = \frac{1}{1+\gamma^*} F_h, \tag{4.16a}$$

$$F_q = F_{q^*} = \frac{\gamma}{L_c\left(1+\gamma^*\right)} F_h \tag{4.16b}$$

and

$$F_\ell = F_r - F_{q^*} = F_r - \frac{\gamma^*}{L_c\left(1+\gamma^*\right)} F_h , \tag{4.16c}$$

where $\gamma^* \equiv \frac{L_c}{c_p}\left(\partial q^* / \partial T\right)_p$. From (4.15), (4.16) and defining, we can write F_{sv} at the top of the PBL as

$$\left(F_{sv}\right)_{B^-} = \beta_{B^-}\left(F_h\right)_{B^-} - \Pi_B \theta_{PBL}\left(F_r\right)_{B^-} \tag{4.17}$$

where $\beta_{B^-} \equiv \left(1+1.608\gamma_{B^-}\Pi_B\theta_{PBL}/L\right)\Big/\left(1+\gamma_{B^-}\right)$. In (4.17),

$$\left(F_r\right)_{B^-} = -E\left(\Delta r\right)_{B^-} = -E\left(q_{B^+} - r_{B^-}\right) \tag{4.18a}$$

and

$$\left(F_h\right)_{B^-} = -E\left(\Delta h\right)_B + \left(\Delta R\right)_B = -E\left(h_{B^+} - h_{B^-}\right) + \left(\Delta R\right)_B . \tag{4.18b}$$

In (4.17a) and (4.18b), $r_{B^-} \equiv r_{L+1}$ and $h_{B^+} \equiv \Pi_B \theta_{B^+} + \Phi_B + Lq_{B^+}$ and $h_{B^-} = h^*_{B^-} \equiv \Pi_B \theta_{B^-} + \Phi_B + Lq^*_{B^-}$. We used (A.3) with $M_B = 0$ of Appendix A in writing (4.18a) and (4.18b). The expression we use for the entrainment rate *E* in (4.18a) will be given later. We write F_{sv} at the bottom of the cloud level

$$\left(F_{sv}\right)_{C^+} \equiv \frac{1}{1+\gamma_C}\left(1 + \frac{1.608\Pi_C\theta_{PBL}\gamma^*_C}{L_c}\right)\left(F_h\right)_C - \Pi_C\theta_{PBL}\left(F_r\right)_C , \tag{4.19}$$

where

$$\left.\begin{aligned}\left(F_h\right)_C &= \frac{\left(F_h\right)_S\left(p_C - p_B\right) + \left(F_h\right)_{B^-}\left(p_S - p_C\right)}{p_S - p_B} \\ \left(F_r\right)_C &= \frac{\left(F_r\right)_S\left(p_C - p_B\right) + \left(F_r\right)_{B^-}\left(p_S - p_C\right)}{p_S - p_B}\end{aligned}\right\}. \tag{4.20}$$

Note that F_{sv} is discontinuous across condensation level while F_h and F_r are continuous (see Fig. 8).

Within the subcloud layer ($p>p_C$):

$$F_{sv} \equiv F_s + 0.608\Pi\theta F_q\,, \tag{4.21}$$

where

$$\left.\begin{aligned}F_s &= F_h - L_c F_r \\ F_q &= F_r\end{aligned}\right\} \tag{4.22}$$

Using (4.21) and (4.22), F_{sv} at the condensation level and the surface are

$$\left(F_{sv}\right)_{C^-} \equiv \left(F_h\right)_C + \left(0.608\Pi_C\theta_{PBL} - L_c\right)\left(F_r\right)_C\,. \tag{4.23}$$

and

$$\left.\begin{aligned}\left(F_{sv}\right)_S &= \left(F_h\right)_S + \left(0.608\,\Pi_S\,\theta_{PBL} - L_c\right) \\ \left(F_h\right)_S &= \Pi_S\left(F_\theta\right)_S + 0.608\,\Pi_S\,\theta_{PBL}\left(F_r\right)_S\end{aligned}\right\}, \tag{4.24}$$

respectively. In (4.23), $\left(F_h\right)_C$ and $\left(F_r\right)_C$ are given by (4.20). In (2.24), $\left(F_r\right)_S \equiv \left(F_q\right)_S$.

Buoyancy generation for this case can be written as

$$\mathcal{B} \approx \kappa\left[\left(F_{sv}\right)_S + \left(F_{sv}\right)_{C^-}\right]\left(p_S - p_C\right)\Big/\left(p_S + p_C\right)$$

$$+\kappa\left[\left(F_{sv}\right)_{C^+}+\left(F_{sv}\right)_{B^-}\right]\left(p_C-p_B\right)\Big/\left(p_C+p_B\right). \tag{4.25}$$

Following Randall, Branson, Zhang, Moeng and Krasner (unpublished manuscript), we calculate the entrainment rate for a cloud topped PBL by

$$E\approx\frac{b_1\rho_{PBL}\sqrt{\tilde{e}_{PBL}}+\hat{b}_2\beta g\left[\dfrac{(\delta z)_{PBL}}{\tilde{e}_{PBL}}\right]\dfrac{(\Delta R)_B}{\Pi_B\theta_{PBL}}}{1+b_2 g\left[\dfrac{(\delta z)_{PBL}}{e_{PBL}}\right]\dfrac{\Delta s_v-\Delta s_{v_{crit}}}{\Pi_B\theta_{PBL}}}, \tag{4.26}$$

where b_1 is a constant and, $\hat{b}_2$ is defined by $b_2\left(1-e^{-\lambda\tilde{e}_{PBL}}\right)$ with two constants b_2 and λ. In the model, b_2 is multiplied by $\left(1-e^{-\lambda\tilde{e}_{PBL}}\right)$, where λ is arbitrarily chosen as $0.1/e_{min}$ to guarantee that $E\to 0$ as $\tilde{e}_{PBL}\to 0$. The constants b_1 and b_2 must be chosen to satisfy $b_1/b_2=2kC/(1-k)$ and currently $b_1\approx 0.4$ and $b_2\approx 0.8$ are chosen. The effect of cloud-top entrainment instability is included in (4.26) through the term with $\Delta s_v-\Delta s_{v_{crit}}$, where $\left(\Delta s_v\right)_{crit}\equiv\left[\dfrac{L-1.608\Pi_B\theta_{B^+}}{\left(1+\gamma_{B^+}\right)}\right]\times\left[q^*\left(\Pi_B\theta_{B^+}/c_p,p_B\right)-q_{B^+}\right]$. Finally we assume $\left(\Delta R\right)_B\approx\left(R_{LW}\right)_{B^+}$, where R_{LW} is the longwave radiation flux. The entrainment formulation given by (7.26) is one of the formulas discussed in Stevens' (2002) comparison paper. The original derivation of (4.26) is discussed in details in Appendix D.

e. Determination of shear generation

We discretize the shear generation (4.5) in the discrete system as

$$\mathrm{S}\approx\alpha_{\mathrm{s}}\left\{\left|\left(\mathbf{F}_{\mathrm{v}}\right)_S\right|\cdot\left|\mathbf{v}_M\right|+\tfrac{1}{2}E\left|\Delta\mathbf{v}\right|_B^2\right\}, \tag{4.27}$$

where *M* denotes the lowest layer of PBL. In (4.27), we introduce a weighting factor α_S to limit the shear generation for buoyancy driven deep PBL while to keep it for a shallow PBL as

$$\alpha_S \equiv \left[\frac{|L|}{|L| + \varepsilon(z_B - z_S)} \right]^3, \tag{4.28}$$

where *L* is the Monin-Obukov length and ε is chosen as 10. The Monin-Obukov length *L* is defined by

$$L = (z_M - z_S)/\zeta_M , \tag{4.29}$$

where z_M and z_S are the height of the first model layer and the surface, respectively. In (4.29), ζ_M is determined from

$$\left.\begin{array}{ll} \textit{For a stable boundary layer} & \dfrac{\zeta_M (0.74 + 4.7\zeta_M)}{(1 + 4.7\zeta_M)^2} = (R_i)_M > 0 \\ \textit{For a neutral boundary layer} & \zeta_M = 0 \\ \textit{For an unstable boundary layer} & \zeta_M = (R_i)_M < 0 \end{array}\right\}, \tag{4.30}$$

where

$$(R_i)_M \equiv \frac{g\left[(\tilde{\theta}_v)_S - (\theta_v)_M\right](z_M - z_S)}{(\theta_v)_M |\mathbf{v}|_M^2}. \tag{4.31}$$

In (4.31), $(\tilde{\theta}_v)$ is defined by

$$(\tilde{\theta}_v)_S \equiv \frac{c_p (\tilde{T}_v)_S}{\Pi_S} \approx \frac{c_p T_G \left[1 + 0.608 (RH)_S q^*(T_G, p_S)\right]}{\Pi_S}, \tag{4.32}$$

where T_G is the ground temperature and $(RH)_S$ is the relative humidity near the surface approximately given by $(RH)_S \approx (RH)_{M+1/2} \equiv q_{M+1/2} / q^*(T_S, p_S)$, where $q_{M+1/2} \equiv r_M$ for $r_M < q^*(T_S, p_S)$ and $q_{M+1/2} \equiv q^*(T_S, p_S)$ for $r_M \geq q^*(T_S, p_S)$.

Determination of the PBL precipitation when $p_C > p_S$:

When $p_C > p_S$, where p_C is defined by (4.14), the precipitation (drizzle) takes place from the PBL to restore $p_C = p_S$. From (4.14), we can approximately calculate the reduction of total water mixing ratio to achieve $p_C = p_S$ from

$$\delta r_{PBL} \approx \left(q_S^* - q_{B0}^*\right) \frac{p_C - p_S}{p_S - p_B}, \tag{4.33}$$

Using δr_{PBL} calculated from (4.33), the precipitation rate is determined from

$$P = -\delta r_{PBL} \rho_{PBL} (\delta z)_{PBL} (\delta t). \tag{4.34}$$

where (δt) is the time interval used in the integration. The raindrop generation can be distributed to the layers of PBL (proportional to their liquid water content) following

$$\mathcal{R}_\ell = \frac{\ell_\ell \delta r_{PBL}}{\sum_{\ell=L+1}^{M} \ell_\ell}. \tag{4.34}$$

Unstable PBL top (dry case):

If $\theta_{PBL} > \theta_{B^+}$, it is assumed that the entrainment rate *E* increases until the instability is

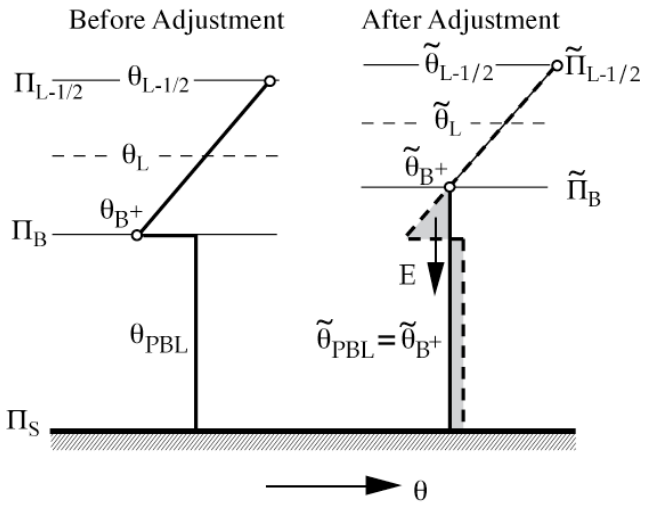

Fig. 9. Treatment of the unstable PBL-top.

eliminated (see Fig. 9). The required entrainment rate E to eliminate the instability in a single time step δt is

$$E = \frac{p_B - \tilde{p}_B}{g\delta t}. \tag{4.35}$$

where $\tilde{p}_B$ can be determined from the following two equations through an iteration

$$\tilde{\Pi}_B \equiv \Pi_B - \left(\Pi_B - \Pi_{L-1/2}\right) \times \left(\tilde{\theta}_{PBL} - \theta_{B^+}\right) \Big/ \left(\theta_{L-1/2} - \theta_{B^+}\right), \tag{4.36}$$

and

$$\tilde{\theta}_{PBL} \equiv \frac{(p_S - p_B)\theta_M - \frac{1}{2}(p_B - \tilde{p}_B)\theta_{B^+}}{p_S - \tilde{p}_B + \frac{1}{2}(p_B - \tilde{p}_B)}. \tag{4.37}$$

It is assumed that potential energy released during the adjustment will contribute to turbulence kinetic energy following

$$\delta e_{PBL} \equiv \frac{(PE)_{PBL} + (PE)_{B^+} - (\tilde{PE})_{PBL}}{p_S - \tilde{p}_B}, \tag{4.38}$$

where $(PE)_{PBL}$ and $(\tilde{PE})_{PBL}$ are the potential energy of the PBL before and after adjustment, and $(PE)_{B^+}$ is the potential energy of the entrained air during the adjustment. $(PE)_{PBL}$ and $(PE)_{B^+}$ can be calculated from

$$(PE)_{PBL} \equiv \frac{c_p \theta_{PBL}}{g\, p_o^{\kappa}} \left[\frac{1}{\kappa+1} \left(p_B^{\kappa+1} - p_S^{\kappa+1} \right) - \left(p_S^{\kappa} p_B - p_S^{\kappa} p_S \right) \right] \qquad (4.39a)$$

and

$$(PE)_{B^+} \equiv \frac{c_p \left(\theta_{B^+} + \tilde{\theta}_{PBL} \right)}{2g\, p_o^{\kappa}} \left[\frac{1}{\kappa+1} \left(\tilde{p}_B^{\kappa+1} - p_B^{\kappa+1} \right) - \left(p_B^{\kappa} \tilde{p}_B - p_B^{\kappa} p_B \right) \right] + z_B \left(p_B - \tilde{p}_B \right), \quad (4.39b)$$

respectively. These expressions for PE are obtained from $PE \equiv g \int_{z=z_1}^{z_2} \rho\, z\, dz = -\int_{p=p_1}^{p_2} z\, dp$ and $z = z_1 + \theta_1 \left(\Pi_1 - \Pi \right) / g$. In derivation of (4.39b), we assume that the origin of the entrained air is the lower half of the layer *L* has the properties of the L to be entrained. Then, the potential temperature of entrained air is $\theta = \left(\theta_{B^+} + \tilde{\theta}_{PBL} \right) / 2$. In the model, we apply "soft" adjustments obtained by multiplying E and δe_{PBL} by $\delta t / \tau_{dca}$, where τ_{dca} is the adjustment time scale typically 1 hour.

5. Formulation of the effects of small eddies

In the hybrid parameterization being described here, we determine the turbulent fluxes due to small eddies through a K-closure formulation based on Troen and Mahrt (1986) and Holtslag and Boville (1993). In our application here, we have replaced the PBL mean velocity scales used by the original formulation by the square root of TKE to solely represent the effects of small eddies generated through a cascade process from the convective large eddies.

a. General aspects of K-closure formulation

For an arbitrary quantity ψ (moist static energy, *h* and/or total water mixing ratio, *r*), turbulent fluxes due to small eddies are formulated as

$$\tilde{F}_{\psi} \equiv -\rho K_{\psi}\left(\frac{\partial \psi}{\partial z} - \gamma_{\psi}\right). \tag{5.1}$$

In (5.1), the diffusion coefficient is defined as

$$K_{\psi} \equiv k\, w_{\psi}\, z\left(1 - \frac{z}{(\delta z)_{PBL}}\right)^{2}, \tag{5.2}$$

where *k* is the Von Karman constant and w_{ψ} a characteristic turbulent velocity scale. In (5.1), the transport term is given by $\gamma_{\psi} \equiv a\left(\overline{\psi' \mathrm{w}'}\right)_{S} \Big/ \sqrt{e_{PBL}}\,(\delta z)_{PBL}$, where *a* is a coefficient and $\left(\overline{\psi' w'}\right)_{S}$ the surface flux of ψ. In the cloud layer, a large value is used for the diffusion coefficient instead of (5.2).

b. Determination of fluxes in a dry PBL or in the subcloud layer

In this subsection, we describe the determination of the turbulent fluxes for different type of PBL regimes.

1. *For the surface layer of a stable or neutral PBL*:

In this regime, the surface fluxes are downward $\left(\overline{\psi' \mathrm{w}'}\right)_S \le 0$. Within the lowest portion of the PBL [$z/(\delta z)_{PBL} \le 0.1$], the characteristic turbulent velocity scale for heat and moisture is given by

$$\mathrm{w}_h = \frac{u_*}{\phi_h}, \tag{5.3}$$

where $u_* \equiv \left(F_{\mathrm{v}}/\rho\right)_S$ and ϕ_h is the dimensionless vertical temperature gradient given by

$$\phi_h \equiv 1 + 5\frac{z}{L} \quad \text{for} \quad 0 \le z/L \le 1 \tag{5.4a}$$

and

$$\phi_h \equiv 5 + \frac{z}{L} \quad \text{for} \quad z/L > 1\ , \tag{5.4b}$$

where L is the Monin-Obukov scale defined by $L \equiv \dfrac{-u_*^3}{k\left(g/\theta_{vS}\right)\left(\overline{\theta_v' \mathrm{w}'}\right)_S}$

where $\left(\overline{\theta_v' \mathrm{w}'}\right)_S \equiv \left(F_{\theta_v}/\rho\right)_S = \left(F_\theta/\rho\right)_S + 0.608\,\theta_S\left(F_r/\rho\right)_S$. The characteristic turbulent velocity scale for momentum w_m is assumed identical to w_h. For this case, it is assumed that there is to transport with the small eddies, $\gamma_\psi \equiv 0$.

2. *For the outer PBL of a stable or neutral PBL*:

Within the outer PBL [$z/(\delta z)_{PBL} > 0.1$], the characteristic turbulent velocity scale for heat and moisture is given by

$$\mathrm{w}_h = \alpha \sqrt{e_{PBL}} \tag{5.5}$$

where

$$\left.\begin{array}{ll} \alpha = 1 & \text{if } \sqrt{e_{PBL}} \le \dfrac{u_*}{\phi_h(z_a)} \\ \alpha = \dfrac{u_*}{\phi_h(z_a)\sqrt{e_{PBL}}} & \text{if } \sqrt{e_{PBL}} > \dfrac{u_*}{\phi_h(z_a)} \\ z_a \equiv 0.1(\delta z)_{PBL} & \end{array}\right\}. \tag{5.6}$$

In (5.6), the dimensionless vertical temperature gradient ϕ_h is calculated from (5.4a) and (5.4b). The characteristic turbulent velocity scale for momentum w_m is assumed identical to w_h. For this case, it is assumed that there is to transport with the small eddies, $\gamma_\psi \equiv 0$.

3. *For the surface layer of an unstable PBL*:

In this regime, the surface fluxes are upward $\left(\overline{\psi' \mathrm{w}'}\right)_S > 0$. Within the lowest portion of the PBL [$z/(\delta z)_{PBL} \le 0.1$], the characteristic turbulent velocity scales for heat, moisture and momentum are given by

$$\mathrm{w}_h = \frac{u_*}{\phi_h} \text{ and } \mathrm{w}_m = \frac{u_*}{\phi_m} \tag{5.7}$$

where

$$\phi_h \equiv \left(1-15\frac{z}{L}\right)^{-1/2} \text{ and } \phi_m \equiv \left(1-15\frac{z}{L}\right)^{-1/3}. \tag{5.8}$$

where L is the Monin-Obukov scale defined by $L \equiv \dfrac{-u_*^3}{k\left(g/\theta_{vS}\right)\left(\overline{\theta_v' \mathrm{w}'}\right)_S}$

where $\left(\overline{\theta_v' \mathrm{w}'}\right)_S \equiv \left(F_{\theta_v}/\rho\right)_S = \left(F_\theta/\rho\right)_S + 0.608\,\theta_S\left(F_r/\rho\right)_S$. For this case, it is assumed that there is to transport with the small eddies, $\gamma_\psi \equiv 0$.

4. *For the outer PBL of an unstable PBL*:

Within the outer PBL [$z/(\delta z)_{PBL} > 0.1$], the characteristic turbulent velocity scale for heat and moisture is given by

$$w_h = \sqrt{e_{PBL}}\,. \tag{5.9}$$

and the characteristic turbulent velocity scale for momentum is given by

$$\mathrm{w}_m = P_r\,\mathrm{w}_h\,, \tag{5.10}$$

where the Prandl number P_r is determined from

$$\left.\begin{array}{lll} P_r \equiv & 1.0 & for \quad 0 > \mathcal{B}/\mathcal{S} \\ P_r \equiv & -0.04\left(\mathcal{B}/\mathcal{S}\right)+1.0 & for \quad 0 \le \mathcal{B}/\mathcal{S} \le 10 \\ P_r \equiv & 0.6 & for \quad \mathcal{B}/\mathcal{S} > 10 \end{array}\right\}. \tag{5.11}$$

The formula given by (5.11) is a simplification of the relationship schematically shown in Fig. 10.

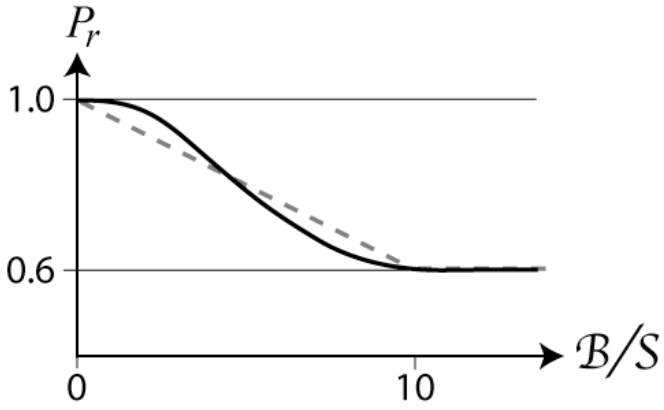

Fig. 10. A schematic plot of Prantl number versus Buoyancy/Shear generations ($\mathcal{B}/S$).

For this case, the transport term for the heat and moisture is given by

$$\gamma_h \equiv a' \frac{\left(\overline{\psi' w'}\right)_S}{w_h \left(\delta z\right)_{PBL}} . \tag{5.12}$$

Here we use $a' \approx 0.75$, which is a fraction of that suggested by Troen and Mahrt (1986). For momentum, $\gamma_m \equiv 0$ is used.

6. Summary and discussions

In this technical report, we have presented a detailed description of the new PBL parameterization incorporated into the UCLA-AGCM.

The formulation of PBL processes remains one of the major unsolved problems in atmospheric general circulation modeling due complicated physical processes involved. A detailed simulation of the behavior and structure of the PBL would require an extremely high vertical resolution with a complex parameterization of turbulence interacting with cloud microphysics and radiation. This is usually impractical in most applications of a GCM. In this paper, we have presented a parameterization to simplify formulation of the PBL processes using a bulk approach. In this parameterization, we designate multiple variable-depth layers next to the lower boundary as the PBL. The depth of the entire PBL is predicted trough a mass budget equation including contributions of the parameterized mass entrainment (detrainment) into (out of) the PBL through the PBL top. To incorporate the variable-depth PBL into a GCM, a system of two coordinates is chosen as the vertical coordinate, one for the PBL and the other for the free atmosphere sharing the PBL top as a coordinate surface. The temperature, moisture and wind fields within the PBL are predicted using the surface fluxes and the fluxes associated with the entrainment (or detrainment) through the PBL top and diffusive fluxes between the layers. For this purpose, a hybrid parameterization is used, one of which is the bulk parameterization and the other a K-closure formulation. The bulk parameterization is used in formulating turbulence fluxes due to convectively active large eddies, PBL-top entrainment (or detrainment), surface fluxes and PBL clouds, which is based on the predicted bulk TKE. The K-closure formulation based on a bulk Richardson number is used for the effects of diffusive small eddies cascaded from the convective large eddies. With this hybrid

parameterization, simulated profiles in the PBL are allowed to deviate from well-mixed profiles, although the deviations are small for thermodynamic conservative variables when TKE is large.

We have incorporated the multi-layer PBL parameterization into our generalized vertical coordinate model using a hybrid $\theta - \sigma$ coordinate (Konor and Arakawa, 1997). Motivated by the encouraging results obtained by this model, the multi-layer parameterization has also been incorporated into the UCLA GCM. We will present the performance of the multi-layer PBL in climate simulations with the GCM in a forthcoming paper.

While our current multi-layer PBL parameterization significantly advances the parameterizations based on single-layer mixed-layer approach (e.g. Suarez et al., 1983), we are planning future improvements in

1) the entrainment formulation,
2) the K-closure formulation specifically designed to treat the diffusion within the subcloud layer (e.g. van Meijgaard and Ulden, 1998)
3) the prediction of the TKE for each PBL layer (e.g. Bechtold et al., 1992),
4) the parameterization of convection within the PBL by including an Arakawa-Schubert type cumulus scheme also operating in the PBL, and
5) the parameterization of horizontal structure within the PBL by including a version of the mass-flux model (e.g. Lappen and Randall, 2001a-c).

APPENDIX A

Discrete Pressure Gradient Force Term

Here we discuss the derivation of the pressure gradient force for the layers within the PBL. The derivation procedure is based on the one followed by Suarez et al. (1983), in which each layer is assumed internally well mixed. As far as the pressure gradient force is concerned, the single layer version of the multi layer model becomes identical to the traditional model described by Suarez et al. (1983).

The pressure on the coordinate surfaces within the PBL can be defined by

$$p = p_S + m\left(\sigma - \sigma_S\right). \tag{A.1}$$

Note that the subscript PBL is omitted in m_{PBL}. The pressure gradient force on the sigma surfaces is

$$-\left(\nabla\Phi\right)_p = -\nabla_\zeta\Phi + \frac{\partial\Phi}{\partial p}\nabla_\zeta p\,. \tag{A.2}$$

If we assume that the individual PBL layers are internally vertically well mixed, we can write the mean pressure gradient force (A.2) for the layer ℓ as

$$-\left(\nabla_p\Phi\right)_\ell = \frac{1}{\sigma_{\ell+1/2}-\sigma_{\ell-1/2}}\int_{\sigma_{\ell-1/2}}^{\sigma_{\ell+1/2}}\left(-\nabla_\sigma\Phi\right)d\sigma + \frac{1}{\sigma_{\ell+1/2}-\sigma_{\ell-1/2}}\int_{\sigma_{\ell-1/2}}^{\sigma_{\ell+1/2}}\left(\frac{\partial\Phi}{\partial p}\nabla_\sigma p\right)d\sigma\,. \tag{A.3}$$

Then using (A.1) and defining

$$-\nabla\Phi_\ell \equiv \frac{1}{\sigma_{\ell+1/2}-\sigma_{\ell-1/2}}\int_{\sigma_{\ell-1/2}}^{\sigma_{\ell+1/2}}\left(-\nabla_\sigma\Phi\right)d\sigma \tag{A.4}$$

in (A.3), we can rewrite (A.3) as

$$-\left(\nabla_p \Phi\right)_\ell = -\nabla\Phi_\ell + \frac{1}{\sigma_{\ell+1/2} - \sigma_{\ell-1/2}} \int_{\sigma_{\ell-1/2}}^{\sigma_{\ell+1/2}} \left\{ \frac{\partial \Phi}{\partial p} \nabla_\sigma \left[p_S + m\left(\sigma - \sigma_S\right) \right] \right\} d\sigma \,. \qquad \text{(A.5)}$$

Using the hydrostatic equation given by

$$\frac{\partial \Phi}{\partial p} = \frac{1}{m} \frac{\partial \Phi}{\partial \sigma} \,, \qquad \text{(A.6)}$$

in (A.5), we further rewrite (A.5) as

$$-\left(\nabla_p \Phi\right)_\ell = -\nabla\Phi_\ell + \frac{1}{m\left(\sigma_{\ell+1/2} - \sigma_{\ell-1/2}\right)} \left(\nabla p_S\right) \int_{\sigma_{\ell-1/2}}^{\sigma_{\ell+1/2}} \frac{\partial \Phi}{\partial \sigma} d\sigma$$

$$+ \frac{1}{m\left(\sigma_{\ell+1/2} - \sigma_{\ell-1/2}\right)} \left(\nabla m\right) \int_{\sigma_{\ell-1/2}}^{\sigma_{\ell+1/2}} \frac{\partial \Phi}{\partial \sigma} \sigma \, d\sigma - \frac{1}{m\left(\sigma_{\ell+1/2} - \sigma_{\ell-1/2}\right)} \sigma_S \left(\nabla m\right) \int_{\sigma_{\ell-1/2}}^{\sigma_{\ell+1/2}} \frac{\partial \Phi}{\partial \sigma} d\sigma \,. \qquad \text{(A.7)}$$

If we use

$$\Phi_{\ell+1/2} - \Phi_{\ell-1/2} = \int_{\sigma_{\ell-1/2}}^{\sigma_{\ell+1/2}} \frac{\partial \Phi}{\partial \sigma} d\sigma \,, \qquad \text{(A.8)}$$

$$\int_{\sigma_{\ell-1/2}}^{\sigma_{\ell+1/2}} \frac{\partial \Phi}{\partial \sigma} \sigma \, d\sigma = \Phi_{\ell+1/2} \sigma_{\ell+1/2} - \Phi_{\ell-1/2} \sigma_{\ell-1/2} - \Phi_\ell \left(\sigma_{\ell+1/2} - \sigma_{\ell-1/2} \right) \qquad \text{(A.9)}$$

and

$$\nabla p_S = \nabla p_B - \left(\sigma_B - \sigma_S\right) \nabla m \,, \qquad \text{(A.10)}$$

which is obtained by applying del operator to (A.1), we obtain the pressure gradient force for layer ℓ of the PBL is

$$-\left(\nabla_p \Phi\right)_\ell = -\nabla\Phi_\ell - \frac{1}{m\left(\sigma_{\ell+1/2} - \sigma_{\ell-1/2}\right)}\left(\Phi_{\ell-1/2} - \Phi_{\ell+1/2}\right)\left(\nabla p_B\right)$$

$$-\frac{(\nabla m)}{m\left(\sigma_{\ell+1/2} - \sigma_{\ell-1/2}\right)}\left[\sigma_{\ell+1/2}\left(\Phi_\ell - \Phi_{\ell+1/2}\right) + \sigma_{\ell-1/2}\left(\Phi_{\ell-1/2} - \Phi_\ell\right) - \sigma_B\left(\Phi_{\ell-1/2} - \Phi_{\ell+1/2}\right)\right]. \quad \text{(A.11)}$$

APPENDIX B

Derivation of the discrete budget equations for the PBL layers

Let us consider a general budget equation for an arbitrary quantity ψ applied to the layers of the PBL given by

$$\frac{\partial(m\psi)_{L+1}}{\partial t} + \nabla\cdot(\psi m\mathbf{v})_{L+1} + \frac{1}{(\delta\sigma)_{L+1}}\left[\psi_{L+3/2}(m\dot{\sigma})_{L+3/2} - \psi_{B^-}(m\dot{\sigma})_{L+1/2}\right]$$

$$= (mS)_{L+1} + \frac{g}{(\delta\sigma)_{L+1}}\left[(F_\psi)_{L+3/2} - (F_\psi)_{B^-}\right], \qquad \text{(B.1a)}$$

and

$$\frac{\partial(m\psi)_\ell}{\partial t} + \nabla\cdot(\psi m\mathbf{v})_\ell + \frac{1}{(\delta\sigma)_\ell}\left[\psi_{\ell+1/2}(m\dot{\sigma})_{\ell+1/2} - \psi_{\ell-1/2}(m\dot{\sigma})_{\ell-1/2}\right]$$

$$= (mS)_\ell + \frac{g}{(\delta\sigma)_\ell}\left[(F_\psi)_{\ell+1/2} - (F_\psi)_{\ell-1/2}\right] \quad \text{for } \ell = L+2,\cdots,M, \qquad \text{(B.1b)}$$

where S is the combined source and sink of ψ. Note that the subscript *PBL* is omitted again in m_{PBL}. In our equations, upward fluxes have positive values. To determine $(F_\psi)_{B^-}$ in (B.1a), we consider the budget equation for the infinitesimally thin transition layer between the free atmosphere and PBL (see Fig. B1).

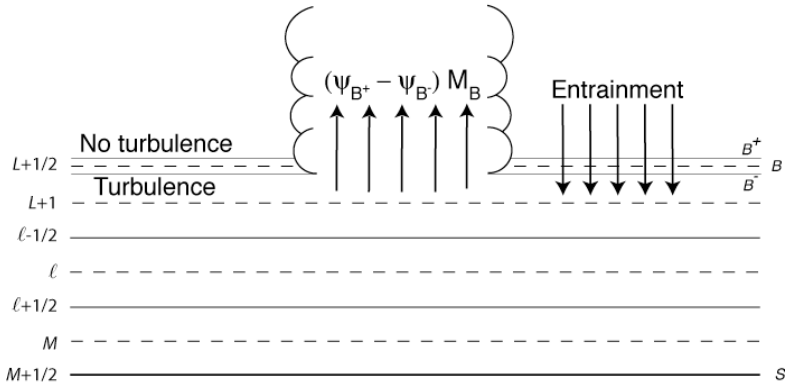

Fig. B1

We assume that the transition layer is so thin that it has no storage. Then, the budget equation for the transition layer becomes

$$0 = -\psi_{B^-} E + \psi_C M_B + \left(F_\psi\right)_{B^-} + \left(R_\psi\right)_{B^-} + \psi_{B^+} E - \psi_C M_B - \left(R_\psi\right)_{B^+}. \qquad \text{(B.2)}$$

On the right hand side of (B.2), the first five and last four terms represent the contributions from B^- and B^+ boundaries of the transition layer, respectively. We assume that the quantity $\psi \equiv \psi_C$ within the cumulus updraft at the top of PBL and there is no turbulent flux at B^+, $\left(F_\psi\right)_{B^+} = 0$. Using $\left(m\dot{\sigma}\right)_B = g\left(E - M_B\right)$ and defining $\left(\Delta R_\psi\right)_B \equiv \left(R_\psi\right)_{B^+} - \left(R_\psi\right)_{B^-}$, we rewrite (A.2) as

$$-\psi_{B^-}\left(m\dot{\sigma}\right)_B + g\left(F_\psi\right)_{B^-} = -\psi_{B^+}\left(m\dot{\sigma}\right)_B - g\left(\psi_{B^+} - \psi_{B^-}\right)M_B + g\left(\Delta R_\psi\right)_B. \qquad \text{(B.3)}$$

Using (B.3) in (B.1a), the budget equation for the uppermost layer of the PBL can be obtain as

$$\frac{\partial\left(m\psi\right)_{L+1}}{\partial t} + \nabla\cdot\left(\psi m\mathbf{v}\right)_{L+1} + \frac{1}{\left(\delta\sigma\right)_{L+1}}\left[\psi_{L+3/2}\left(m\dot{\sigma}\right)_{L+3/2} - \psi_{B^+}\left(m\dot{\sigma}\right)_B\right]$$

$$= \left(mS\right)_{L+1} + \frac{g}{\left(\delta\sigma\right)_{L+1}}\left(F_\psi\right)_{L+3/2} + \frac{g}{\left(\delta\sigma\right)_{L+1}}\left[\left(\psi_{B^+} - \psi_{B^-}\right)M_B - \left(\Delta R_\psi\right)_B\right]. \qquad \text{(B.4)}$$

Now we include turbulent fluxes due to small eddies and effects of the cumulus roots into (B.4) and (B.1b) as

$$\frac{\partial(m\psi)_{L+1}}{\partial t}+\nabla\cdot(\psi m\mathbf{v})_{L+1}+\frac{1}{(\delta\sigma)_{L+1}}\left[\psi_{L+3/2}(m\dot{\sigma})_{L+3/2}-\psi_{B^+}(m\dot{\sigma})_B\right]=(mS)_{L+1}+\frac{g}{(\delta\sigma)_{L+1}}\left(F_\psi\right)_{L+3/2}$$

$$+\frac{g}{(\delta\sigma)_{L+1}}\left[-\left(\tilde{F}_\psi\right)_{L+3/2}+\lambda_{L+1}^{(c)}\left(\psi_{B^+}-\psi_{B^-}\right)M_B-\left(\Delta R_\psi\right)_B\right], \qquad \text{(B.5a)}$$

$$\frac{\partial(m\psi)_\ell}{\partial t}+\nabla\cdot(\psi m\mathbf{v})_\ell+\frac{1}{(\delta\sigma)_\ell}\left[\psi_{\ell+1/2}(m\dot{\sigma})_{\ell+1/2}-\psi_{\ell-1/2}(m\dot{\sigma})_{\ell-1/2}\right]=(mS)_\ell$$

$$+\frac{g}{(\delta\sigma)_\ell}\left[\left(F_\psi\right)_{\ell+1/2}-\left(F_\psi\right)_{\ell-1/2}\right]+\frac{g}{(\delta\sigma)_\ell}\left[-\left(\tilde{F}_\psi\right)_{\ell+1/2}+\left(\tilde{F}_\psi\right)_{\ell-1/2}+\lambda_\ell^{(c)}\left(\psi_{B^+}-\psi_{B^-}\right)M_B\right]$$

for $\ell=L+2,\cdots,M$. (B.5b)

and

$$\frac{\partial(m\psi)_M}{\partial t}+\nabla\cdot(\psi m\mathbf{v})_M-\frac{1}{(\delta\sigma)_M}\psi_{M-1/2}(m\dot{\sigma})_{M-1/2}=(mS)_M$$

$$-\frac{g}{(\delta\sigma)_M}\left(F_\psi\right)_{M-1/2}+\frac{g}{(\delta\sigma)_M}\left[\left(\tilde{F}_\psi\right)_{M-1/2}+\lambda_M^{(c)}\left(\psi_{B^+}-\psi_{B^-}\right)M_B\right]. \qquad \text{(B.5c)}$$

In (B.5a) to (B.5c), the tilde denotes turbulent fluxes due to small eddies. Note that $\left(\tilde{F}_\psi\right)_{L+1/2}=\left(\tilde{F}_\psi\right)_{M+1/2}=0$.

Fig. B2 schematically shows the procedure, by which the effects of cumulus roots are included in the budget equations. The procedure is based on the redistribution of the cumulus

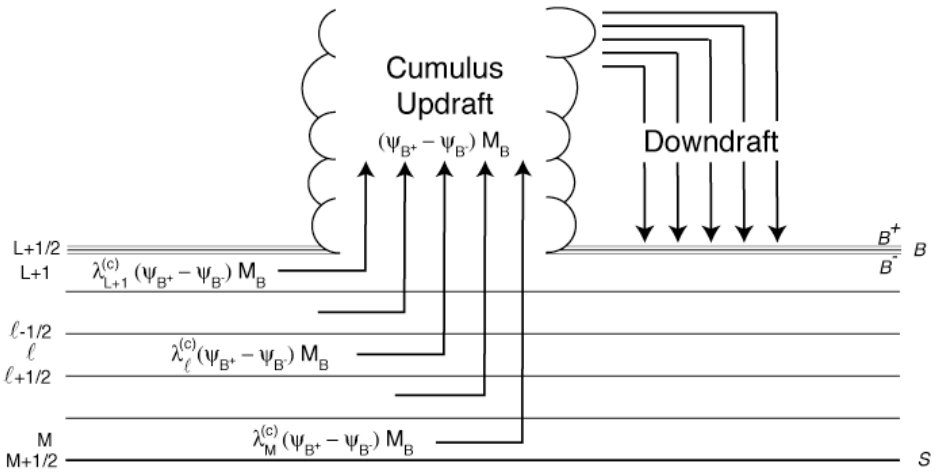

Fig. B2.

mass flux effect $\left(\psi_{B^+} - \psi_{B^-}\right) M_B$ into the all PBL layers through $\lambda_\ell^{(c)} \left(\psi_{B^+} - \psi_{B^-}\right) M_B$,

where $\lambda_\ell^{(c)}$ is a fraction contribution factor satisfying $\sum_{\ell=L+1}^{M} \lambda_\ell^{(c)} = 1$.

APPENDIX C

Derivation of the bulk TKE equation

We can write the mass-weighted TKE equation as

$$\frac{\partial m e_{PBL}}{\partial t} = \frac{mg}{(\delta p)_{PBL}}\left(\mathcal{B} + S - \mathcal{D}\right). \tag{C.1}$$

Note that the horizontal TKE convergence term is neglected. The mass continuity equation for the PBL can be given by

$$\frac{\partial m}{\partial t} = -\nabla \cdot (m\mathbf{v}) + \frac{m}{(\delta p)_{PBL}} gE. \tag{C.2}$$

By multiplying (C.2) by e_{PBL} and using the result in (C.1), we obtain

$$\frac{\partial e_{PBL}}{\partial t} = -\frac{e_{PBL}}{(\delta p)_{PBL}} gE + \frac{g}{(\delta p)_{PBL}}\left(\mathcal{B} + S - \mathcal{D}\right) + \frac{e_{PBL}}{m}\nabla \cdot (m\mathbf{v}). \tag{C.3}$$

APPENDIX D

Entrainment Closure

The formulation discussed here was first implemented by Krasner (1993) in a one-dimensional model and have been recently published by Randall and Schubert (2004). Here we repeat the discussion for convenience.

a. Dry clear PBL

The entrainment parameterization follows the ideas of Breidenthal and Baker (1985), Siems et al. (1990) and Breidenthal (1989). The entrainment rate can be given by

$$E = \frac{b_1 \rho_B \sqrt{e_{PBL}}}{1 + b_2 R_{i\Delta}} . \tag{D.1}$$

Here b_1 and b_2 are assumed to be constants, and the relevant Richardson number is

$$R_{i\Delta} \equiv \frac{g\left(\Delta\theta_v\right)_B \left(\delta z\right)_{PBL}}{\theta_B e_{PBL}} . \tag{D.2}$$

To determine b_1 and b_2, we first consider the strong inversion (or highly stable) case. In this case $b_2 R_{i\Delta} >> 1$, and (D.1) becomes

$$E = \frac{b_1 \rho_B \sqrt{e_{PBL}}}{b_2 R_{i\Delta}} . \tag{D.3}$$

Now we require that (D.3) satisfy

$$-\left(F_{\theta_v}\right)_B = k\left(F_{\theta_v}\right)_S , \tag{D.4}$$

where $k \approx 0.2$, under the condition that the entrainment, buoyancy generation and dissipation effects are in a balance yielding no TKE change. Then, using (4.3), we can write

$$\left[\frac{\left(F_{\theta_v}\right)_S + \left(F_{\theta_v}\right)_B}{2}\right]\frac{g(\delta z)_{PBL}}{\theta_S} = C\rho_{PBL}\left(e_{PBL}\right)^{3/2}, \tag{D.5}$$

Here $C \approx 1$ (according to Moeng and Sullivan, 1994). Using (D.4) in (D.5), we find that

$$\left(\frac{1-k}{2}\right)\left(F_{\theta_v}\right)_S \frac{g(\delta z)_{PBL}}{\theta_S} = C\rho_{PBL}\left(e_{PBL}\right)^{3/2}. \tag{D.6}$$

Now using

$$\left(F_{\theta_v}\right)_B = -E\left(\Delta\theta_v\right)_B \tag{D.7}$$

in (D.4), we obtain

$$\left(F_{\theta_v}\right)_S = \frac{E\left(\Delta\theta_v\right)_B}{k}. \tag{D.8}$$

Using (D.8) in (D.6) and after some arrangement, we obtain an alternative equation that determines the entrainment rate as

$$E = \left(\frac{2kC}{1-k}\right)\left(\frac{\rho_{PBL}\sqrt{e_{PBL}}}{\dfrac{g\left(\Delta\theta_v\right)_B(\delta z)_{PBL}}{\theta_S e_{PBL}}}\right). \tag{D.9}$$

A comparison of (D.9) to (D.1) ignoring the difference between θ_S and θ_B yields that

$$\frac{b_1}{b_2} \cong \frac{2kC}{1-k}. \tag{D.10}$$

Since C=1 and k=0.2, we find that $b_1/b_2 \approx 0.5$. Now we consider the neutral case, for which

$$R_{i\Delta} = 0 \tag{D.11}$$

and, therefore,

$$\left(F_{\theta_v}\right)_B = 0\,. \tag{D.12}$$

For this case, (D.1) should be consistent with

$$E = D\rho_B w^*, \tag{D.13}$$

where $D \approx 0.2$ and w^* is the convective velocity scale of Deardorff (1970) in the present notation approximately given by

$$w^* = \left[\frac{g\left(F_{\theta_v}\right)_S (\delta z)_{PBL}}{(\rho\theta)_S}\right]^{1/3}. \tag{D.14}$$

The relation (D.14) is obtained through LES by Deardorff (1974). In this neutral (no-inversion) case, (D.1) becomes

$$E = b_1 \rho_B \sqrt{e_{PBL}}\,. \tag{D.15}$$

A comparison of (D.15) to (D.13) yields that

$$w^* \cong \frac{b_1}{D}\sqrt{e_{PBL}} \tag{D.16}$$

Since $\left(F_{\theta_v}\right)_B = 0$ for the neutral case, (D.5) becomes

$$\left(F_{\theta_v}\right)_S \frac{g(\delta z)_{PBL}}{\rho_{PBL}\theta_S} = 2C\left(e_{PBL}\right)^{3/2}. \qquad \text{(D.17)}$$

Taking advantage of the similarity between (D.17) and (D.14) by ignoring minor differences, we find

$$w^* \cong (2C)^{1/3}\sqrt{e_{PBL}}\,. \qquad \text{(D.18)}$$

Comparing (D.16) to (D.18), we obtain b_1 as

$$b_1 \cong D(2C)^{1/3}. \qquad \text{(D.20)}$$

Since $D \approx 0.2$ and $C \approx 1$, $b_1 \approx 0.25$, so that, $b_2 \approx 0.5$.

b. Smoke-cloud topped PBL

This case considers a PBL topped with smoke cloud, with radiative cooling at its top, but no phase changes. The presence of radiative cooling can affect the entrainment rate through two processes: *i*) it can increase the TKE and ii) it can cool the entraining air, thus making the inversion (PBL-top jump) appear to be weaker that it really is. Through (D.1) and (D.2) the former process is already included in our formulation. Yet the latter needs to be incorporated. The method we use is based on a modification of the inversion strength to reflect the effect of reduced stability due to radiative cooling in the expression for Richardson number given by (D.2).

To do that, we employ a "mass flux" model. According to Randall et al. (1992), in a situation schematically demonstrated in Fig. D1, we can write

$$\left(\psi_d\right)_{B^-} = \chi_E\overline{\psi}_{B^+} + (1-\chi_E)\overline{\psi}_{B^-} + \frac{\chi_E}{E}\int_{z_{B^-}}^{z_{B^+}} \overline{S}_\psi\, dz\,, \qquad \text{(D.20)}$$

Here ψ is an intensive arbitrary quantity, subscript *d* denotes a "downdraft" property, χ_E is a "mixing parameter" given by

$$\chi_E = \frac{\sigma_B E}{M_B}, \tag{D.21}$$

where bar denotes average across updrafts and downdrafts, σ_B is the fractional area covered by updraft, M_B is a convective mass flux, and $\overline{S}_\psi$ is the source or sink of ψ within the inversion (transition) layer.

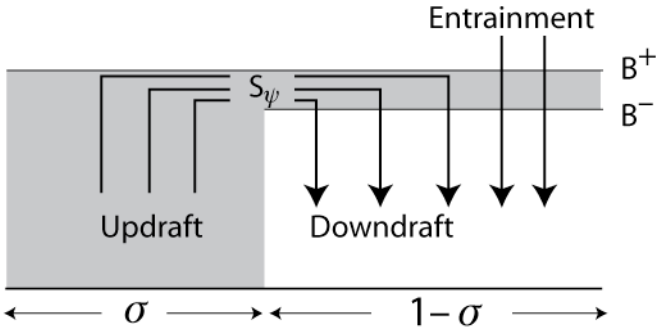

Fig. D1.

If we choose $\psi \equiv h$, then $\int_{z_{B^-}}^{z_{B+}} \overline{S}_\psi \, dz = -(\Delta R)_B$. Note that $(\Delta R)_B > 0$ for radiative cooling. For this case, (D.20) becomes

$$(h_d)_{B^-} = \chi_E \overline{h}_{B^+} + (1-\chi_E)\overline{h}_{B^-} - \frac{\chi_E}{E}(\Delta \overline{R})_B. \tag{D.22}$$

Now we find the expression for the "effective" mean moist static energy at B+ level $\left(\overline{h}_{B^+}\right)_{eff}$ form

$$\chi_E \overline{h}_{B^+} + (1-\chi_E)\overline{h}_{B^-} - \frac{\chi_E}{E}(\Delta \overline{R})_B = \chi_E \left(\overline{h}_{B^+}\right)_{eff} + (1-\chi_E)\overline{h}_{B^-}, \tag{D.23}$$

which immediately becomes

$$\left(\Delta\bar{h}\right)_{eff} = \bar{h}_{B^+} - \frac{\left(\Delta\bar{R}\right)_B}{E}. \tag{D.24}$$

In (D.24), we define $\left(\Delta\bar{h}\right)_{eff} \equiv \left(\bar{h}_{B^+}\right)_{eff} - \bar{h}_{B^-}$. Now we modify the definition of the Richardson number (D.2). We first write

$$\left(\Delta\bar{\theta}_v\right)_{eff} = \left(\Delta\bar{\theta}_v\right)_B - \left(\frac{1}{\Pi_B}\right)\frac{\left(\Delta\bar{R}\right)_B}{E} \tag{D.25}$$

and, then, the Richardson number using (D.25) as

$$\left(R_{i\Delta}\right)_{eff} \equiv \frac{g(\delta z)_{PBL}}{\bar{\theta}_{B^-} e_{PBL}}\left[\left(\Delta\bar{\theta}_v\right)_B - \left(\frac{1}{\Pi_B}\right)\frac{\left(\Delta\bar{R}\right)_B}{E}\right]. \tag{D.26}$$

Using (D.26) in (D.1), we obtain

$$E = \frac{b_1 \rho_{B^-}\sqrt{e_{PBL}}}{1 + b_2 \dfrac{g(\delta z)_{PBL}}{\bar{\theta}_{B^-} e_{PBL}}\left[\left(\Delta\bar{\theta}_v\right)_B - \left(\dfrac{1}{\Pi_B}\right)\dfrac{\left(\Delta\bar{R}\right)_B}{E}\right]}. \tag{D.27}$$

By rearranging the terms in (D.27), we obtained the equation that determines the entrainment rate for a PBL topped by smoke cloud as

$$E = \frac{b_1 \rho_{B^-}\sqrt{e_{PBL}} + b_2 \dfrac{g(\delta z)_{PBL}}{e_{PBL}\Pi_B \bar{\theta}_{B^-}}\left(\Delta\bar{R}\right)_B}{1 + b_2 \dfrac{g(\delta z)_{PBL}\left(\Delta\bar{\theta}_v\right)_B}{\bar{\theta}_{B^-} e_{PBL}}} \tag{D.28}$$

or

$$E = \frac{b_1 \rho_{B^-} \sqrt{e_{PBL}} + b_2 \dfrac{g(\delta z)_{PBL}}{e_{PBL} \Pi_B \bar{\theta}_{B^-}} \left(\Delta \bar{R}\right)_B}{1 + b_2 R_{i\Delta}} \tag{D.29}$$

Under the strong inversion, neglecting "1" in the denominator of (D.28), the entrainment equation (D.29) becomes

$$E = \left(\frac{b_1}{b_2} \rho_{B^-} \frac{\left(e_{PBL}\right)^{3/2}}{g(\delta z)_{PBL}} + \frac{\left(\Delta \bar{R}\right)_B}{\bar{\theta}_{B^-} \Pi_B} \right) \frac{\bar{\theta}_B}{\left(\Delta \bar{\theta}_v\right)_B} . \tag{D.30}$$

c. Water-cloud topped PBL

Now we write

$$\left(r_d\right)_{B^-} = \chi_E \bar{r}_{B^+} + \left(1 - \chi_E\right) \bar{r}_{B^-} . \tag{D.31}$$

Since the air is saturated, we can write

$$\left(s_{vd}\right)_{B^-} - \left(\bar{s}_v\right)_{B^-} = \beta_{B^-} \left[\left(h_d\right)_{B^-} - \bar{h}_{B^-} \right] - \varepsilon_{B^-} L \left[\left(r_d\right)_{B^-} - \bar{r}_{B^-} \right], \tag{D.32}$$

where $\varepsilon_B \equiv \Pi_B \bar{\theta}_B / L$. Using (D.22) in (D.32), we obtain

$$\left(s_{vd}\right)_{B^-} - \left(\bar{s}_v\right)_{B^-} = \beta_{B^-} \left[\chi_E \bar{h}_{B^+} + \left(1 - \chi_E\right) \bar{h}_{B^-} - \frac{\chi_E}{E} \left(\Delta \bar{R}\right)_B - \bar{h}_{B^-} \right] - \varepsilon_{B^-} L \left[\chi_E \bar{r}_{B^+} + \left(1 - \chi_E\right) \bar{r}_{B^-} - \bar{r}_{B^-} \right] \tag{D.33}$$

After some arrangements, (D.33) becomes

$$\left(s_{vd}\right)_{B^-} - \left(\overline{s}_v\right)_{B^-} = \chi_E \left[\beta_{B^-} \left(\Delta\overline{h}\right)_B - \varepsilon_{B^-} L \left(\Delta\overline{r}\right)_B - \beta_{B^-} \frac{\left(\Delta\overline{R}\right)_B}{E} \right]. \qquad \text{(D.34)}$$

Now let us define $\beta_{B^-} \left(\Delta\overline{h}\right)_B - \varepsilon_{B^-} L \left(\Delta\overline{r}\right)_B \equiv \left(\Delta\overline{s}_v\right)_B - \left(\Delta\overline{s}_v\right)_{crit}$ following Randall (1980) and rewrite the right hand side of (D.34) as

$$\chi_E \left[\beta_{B^-} \left(\Delta\overline{h}\right)_B - \varepsilon_{B^-} L \left(\Delta\overline{r}\right)_B - \beta_{B^-} \frac{\left(\Delta\overline{R}\right)_B}{E} \right] \equiv \chi_E \left\{ \left[\left(\Delta\overline{s}_v\right)_B - \left(\Delta\overline{s}_v\right)_{crit} \right] - \beta_{B^-} \frac{\left(\Delta\overline{R}\right)_B}{E} \right\}. \qquad \text{(D.35)}$$

Phase changes and radiative cooling make the inversion seem weaker than it really is. We define $\left(\overline{s}_{vB^+}\right)_{eff}$ by

$$\left(s_{vd}\right)_{B^-} = \chi_E \left(\overline{s}_{vB^+}\right)_{eff} + \left(1 - \chi_E\right)\left(\overline{s}_v\right)_{B^-}, \qquad \text{(D.36)}$$

so that

$$\left(s_{vd}\right)_B - \left(\overline{s}_v\right)_B = \chi_E \left(\Delta\overline{s}_v\right)_{eff}, \qquad \text{(D.37)}$$

where $\left(\Delta\overline{s}_v\right)_{eff} = \left(\overline{s}_{vB^+}\right)_{eff} - \left(\overline{s}_v\right)_{B^-}$. A comparison of (D.35) to (D.37) shows that

$$\left(\Delta\overline{s}_v\right)_{eff} = \left[\left(\Delta\overline{s}_v\right)_B - \left(\Delta\overline{s}_v\right)_{crit} \right] - \beta_{B^-} \frac{\left(\Delta\overline{R}\right)_B}{E}. \qquad \text{(D.38)}$$

To obtain the equation that determines the entrainment rate for this case, we first write the Richardson equation (D.2) in terms of the virtual static energy as

$$R_{i\Delta} \equiv \frac{g\left(\Delta\overline{s}_v\right)_B \left(\delta z\right)_{PBL}}{\Pi_B \overline{\theta}_{B^-} e_{PBL}}. \qquad \text{(D.39)}$$

Then, replacing $\left(\Delta\overline{s}_v\right)_B$ by $\left(\Delta\overline{s}_v\right)_{eff}$ in (D.39) and substituting the result into (D.1), we find

$$E = \frac{b_1 \rho_{B^-} \sqrt{e_{PBL}}}{1 + b_2 \dfrac{g(\delta z)_{PBL}}{\Pi_B \overline{\theta}_{B^-} e_{PBL}} \left\{ \left[\left(\Delta\overline{s}_v\right)_B - \left(\Delta\overline{s}_v\right)_{crit} \right] - \beta_{B^-} \dfrac{\left(\Delta\overline{R}\right)_B}{E} \right\}} \tag{D.40}$$

After some arrangements, we obtain the equation that determines the entrainment rate for a water-cloud topped PBL as

$$E = \frac{b_1 \rho_{B^-} \sqrt{e_{PBL}} + b_2 \dfrac{g(\delta z)_{PBL}}{\Pi_B \overline{\theta}_{B^-} e_{PBL}} \beta_{B^-} \left(\Delta\overline{R}\right)_B}{1 + b_2 \dfrac{g(\delta z)_{PBL}}{\Pi_B \overline{\theta}_{B^-} e_{PBL}} \left[\left(\Delta\overline{s}_v\right)_B - \left(\Delta\overline{s}_v\right)_{crit} \right]} . \tag{D.41}$$

Acknowledgments. We thank Professor David Randall for providing the bulk PBL parameterization used in this study and for his support for the ongoing research. We also thank to Mr. Gabriel Casez Boezio for his valuable help in implementing the PBL parameterization to the UCLA-GCM and performing climate simulations.

References

Arakawa, A., 1969: Parameterization of cumulus clouds. *Proceedings of the WMO/IUGG Symposium on Numerical Weather Prediction*, Tokyo, 1968, Japan Meteorological Agency, IV-8-1 to IV-8-6.

Arakawa, A., and M.J. Suarez, 1983: Vertical differencing of the primitive equations in sigma-coordinates. *Mon. Wea. Rev.*, **111**, 34-45.

Arakawa, A., 2000: A personal prospective on the early development of general circulation modeling at UCLA. In *General Circulation Model Development: Past, Present, and Future*, D. A. Randall Ed, Academic Press, 1-65.

Beljaars, A. and P. Viterbo, 1998: Role of the boundary layer in a numerical weather prediction model. *Clear and Cloudy Boundary Layers*, A. A. M. Holtslag and P. G. Duynkerke, Eds., Elsevier, 287-304.

Bechtold, P., C. Fravalo and J. P. Pinty, 1992: A model of marine boundary-layer cloudiness for mesoscale applications. *J. Atmos. Sci.,* **49**, 1723-1744.

Breidenthal, R. E. and M. B. Baker, 1985: Convection and entrainment across stratified interfaces. *J. Geophys. Res.*, **90D**, 13055-13062.

Breidenthal, R. E., 1992: Entrainment at thin stratified interfaces: The effects of Smith, Richardson and Reynolds numbers. *Phys. Fluids A*, **4**, 2141-2144.

Bretherton, C. S., J. R. McCaa and H. Grenier, 2004: A New Parameterization for Shallow Cumulus Convection and Its Application to Marine Subtropical Cloud-Topped Boundary Layers. Part I: Description and 1D Results. *Mon. Wea. Rev.*, **132**, 864-882.

Deardorff, J. W., 1970: Convective velocity and temperature scales for the unstable planetary boundary layer and for Rayleigh convection. *J. Atmos. Sci.,* **27**, 1211-1213.

Deardorff, J. W., 1972: Parameterization of the planetary boundary layer for use in general circulation models. *Mon. Wea. Rev.,* **100**, 93-106.

Deardorff, J. W., 1974: Three-dimensional numerical study of the height and mean structure of a heated planetary boundary layer. *Bound. Layer Meteor.,* **7**, 81-106.

Gordon, C. T., and W. F. Stern, 1982: A description of the GFDL global spectral model. *Mon. Wea. Rev*, **110**, 625-644.

Grenier, H. and C. S. Bretherton, 2001: A moist PBL parameterization for large-scale models and its application to subtropical cloud-topped marine boundary layers. *Mon. Wea. Rev.*, **129**, 357-377.

Hansen, J., G. Russell, D. Rind, P. Stone, A. Lacis, S. Lebedeff, R. Reudy, and L. Travis, 1983: Efficient three-dimensional global models for climate studies: Model I and II. *Mon. Wea. Rev*, **111**, 609-662.

Holtslag, A. A. M. and C. –H. Moeng, 1991: Eddy diffusivity and countergradient transport in the convective atmospheric boundary layer. *J. Atmos. Sci.,* **48**, 1690-1698.

Holtslag, A. A. M. and B. A. Boville, 1993: Local versus nonlocal boundary-layer diffusion in a global model. *J. Climate,* **6**, 1825-1842.

Konor, C. S., and A. Arakawa, 1997: Design of an atmospheric model based on a generalized vertical coordinate. *Mon. Wea. Rev*., **125**, 1649-1673.

Krasner, R. D., 1993: Further Development and Testing of a Second-Order Bulk Boundary Layer Model. M.S. Thesis, Department of Atmospheric Science, Colorado State University. 131 pp.

Lappen, C.-L. and D. A. Randall, 2001: Toward a unified parameterization of the boundary layer and moist convection. Part I: A new type of mass-flux model. *J. Atmos. Sci.*, **58**, 2021-2036.

Lappen, C.-L. and D. A. Randall, 2001: Toward a unified parameterization of the boundary layer and moist convection. Part III: Simulations of clear and cloudy convection. *J. Atmos. Sci.*, **58**, 2037-2051.

Lappen, C.-L. and D. A. Randall, 2001: Toward a unified parameterization of the boundary layer and moist convection. Part II: Leteral mass exchanges and subplume-scale fluxes. *J. Atmos. Sci.*, **58**, 2052-2072.

Li, J.-J. F., A. Arakawa and C. R. Mechoso, 1999: Revised planetary boundary layer moist processes in the UCLA General Circulation Model. Tenth Symposium on Global Change Studies, 10-15 January 1999, Dallas, Texas, American Meteorological Society.

Lilly, D. K., 1968: Models of cloud-topped mixed layers under a strong inversion. *Quart. J. Roy. Meteor. Soc.*, **94**, 292-309.

Lock, A. P., A. R. Brown, M. R. Bush, G. M. Martin and R. N. B. Smith, 2000: A new boundary layer scheme. PartI: Scheme description and single-column model tests. *Mon. Wea. Rev.*, **128**, 3187-3199.

McCaa, J. R. and C. S. Bretherton, 2004: A New Parameterization for Shallow Cumulus Convection and Its Application to Marine Subtropical Cloud-Topped Boundary Layers. Part II: Regional Simulations of Marine Boundary Layer Clouds. *Mon. Wea. Rev.*, **132**, 883-896.

Moeng, C. –H. and P. P. Sullivan, 1994: A comparison of shear- and buoyancy-driven planetary boundary layer flows. *J. Atmos. Sci.*, **51**, 999-1022.

Randall, D. A., 1976: The interaction of the planetary boundary layer with large-scale circulations. Ph.D. Thesis, Department of Atmospheric Sciences, UCLA, 247 pp.

Randall, D. A., Q. Shao, and C. –H. Moeng, 1992: A second-order bulk boundary layer model. *J. Atmos. Sci.*, **49**, 1903-1923.

Randall, D. A., M. A. Branson, C. Zhang, C.-H. Moeng and R. D. Krasner, 1998: An updated bulk boundary layer parameterization. *Unpublished*.

Randall, D. A., R. D. Harshvardhan, D. A. Dazlich and T. G. Corsetti, 1989: Interactions among Radiation, Convective, and Large-Scale Dynamics in a General Circulation Model, *J. Atmos. Sci*, **46**, 1943-1970.

Randall, D. A., and W. H. Schubert, 2004: Dreams of Stratocumulus sleeper. In Atmospheric Turbulence and Mesoscale Meteorology. Edited by E. Fedorovich, R. Rotunno and B. Stevens. *Cambridge University Press*. 279 pp.

Siebesma, A. P., P. M. M. Soares and J. Teixeira, 2007: Interactions among Radiation, Convective, and Large-Scale Dynamics in a General Circulation Model, *J. Atmos. Sci*, **64**, 1230-1248.

Siems, S. T., C. S. Bretherton, M. B. Baker S. Shy, and R. E. Breidenthal, 1990: Buoyancy reversal and cloud top instability. *Quart. J. Roy. Meteor. Soc.*, **116**, 705-739.

Soares, P. M. M., P. M. A. Miranda, A. B. Siebesma and J. Teixeira., 2004: An eddy-diffusivity/mass-flux parameterization for dry and shallow cumulus convection. *Quart. J. Roy. Meteor. Soc.*, **130**, 3365-3383.

Stevens, B., 2002: Entrainment in stratocumulus-topped mixed layers. *Quart. J. Roy. Meteor. Soc.*, **128**, 2663-2690.

Suarez, M. J., A. Arakawa and D .A. Randall, 1983: The parameterization of the planetary boundary layer in the UCLA general circulation model: formulation and results. *Mon. Wea. Rev.*, **111**, 2224-2243.

Sud, Y. C. and G. K. Walker, 1992: A review of recent research on improvement of physical parameterizations in the GLA GCM. In Physical Processes in atmospheric models, D. R. Sikka and S.S. Singh (eds.), Wiley Eastern Ltd., New Delhi, 422-479.

Takacs, L. L., 1985: A two-step scheme for the advection equation with minimized dissipation and dispersion errors. *Mon. Wea. Rev.*, **113**, 1050-1065.

Troen, I., and L. Mahrt, 1986: A simple model of the atmospheric boundary layer: Sensitivity to surface evaporation. *Boun.-Layer Meteor.*, **37**, 129-148.

van Meijgaard, E. and A. P. van Ulden, 1998: A first-order mixing and condensation scheme for nocturnal stratocumulus. *Atmos. Res.*, **45**, 253-273.

Wyngaard, J. C., and C.-H. Moeng, 1990: A global survey of PBL models used within GCMs. *In proceedings of PBL model evaluation workshop: European Centre for Medium-Range Forecasts,* P. Taylor and J. C. Wyngaard (Eds.), 14-15 August, 1989, Reading, U.K., World Climate Research Program Series 42, WMO/TD 378.

Zhang, C., D. A. Randall, C. –H. Moeng, M. Branson, K. A. Moyer, and Q. Wang, 1996: A surface flux parameterization based on the vertically averaged turbulence kinetic energy. *Mon. Wea. Rev* ., **124**, 2521-2536.